~~On the regional-scale streamflow variability using flow duration curve~~ On the regional-scale variability of flow duration curves in Peninsular India

Pankaj Dey[1], Jeenu Mathai[2], Murugesu Sivapalan[3,4] and Pradeep. P. Mujumdar[5,6]

[1]Department of Hydrology, Indian Institute of Technology, Roorkee, India

[2]Marine Geoscience Group, National Centre for Earth Science Studies, Thiruvananthapuram, India

[3]Department of Civil and Environmental Engineering, University of Illinois at Urbana-Champaign, Urbana, IL, USA

[4]Department of Geography and Geographic Information Science, University of Illinois at Urbana-Champaign, Urbana, IL, USA

[5]Department of Civil Engineering, Indian Institute of Science, Bangalore, India

[6]Interdisciplinary Centre for Water Research, Indian Institute of Science, Bangalore, India

Correspondence to: Pankaj Dey (pdey609@gmail.com)

Abstract. ~~As each catchment responds uniquely, even if they appear similar, formulating generalizable hypotheses and using routinely used signatures of catchment similarity to examine streamflow variability can be difficult. Flow Duration Curve (FDC), a concise portrayal of streamflow variability at a specific gauging station, can provide insights into hydroclimatic and landscape processes occurring at a wide range of space and time scales that govern flow regimes in a region. This study explores the suitability of partitioning of annual streamflow FDC into seasonal FDCs, and total streamflow FDC into fast and slow flow FDCs to unravel the process controls on FDCs at a regional scale, with application to low gradient rivers flowing east from the Western Ghats of Peninsular India. The focus is on investigation of the controls of common regional landscape features (in space) and seasonal climatic (in time) variations on regional variations of the FDC. Findings of the study indicate that bimodal rainfall seasonality and higher fraction of moderate to good groundwater potential zones explains the higher contribution of slow flow to total flow across north-south gradient of the region. Shapes of fast and slow FDCs are controlled by recession parameters revealing the role of climate seasonality and geologic profiles, respectively. A systematic spatial variation across north-south gradient is observed highlighting the importance of coherent functioning of landscape-hydroclimate settings in imparting distinct signature of streamflow variability. The framework is useful to discover the role of time and process controls on streamflow variability in a region with seasonal hydroclimatology and hydro-geologic gradients.~~As each catchment responds uniquely, even when appearing similar, formulating generalizable hypotheses and using routinely employed signatures of catchment similarity to examine streamflow variability can be challenging. The Flow Duration Curve (FDC), offering a concise portrayal of streamflow variability at a specific gauging station, provides insights into hydroclimatic and landscape processes operating across a broad range of spatial and temporal scales that govern flow regimes in a region. This study delves into the controls of streamflow variability in Peninsular India, specifically focusing on low-gradient rivers flowing east from the Western Ghats. The novelty of the study lies in partitioning streamflow into three time-wise categories (non-monsoon, southwest monsoon, northeast monsoon)

39 and two process-related partitions (fast flow and slow flow) using FDCs. The methodology enables a detailed
40 examination of the contributions of each season and process to the overall annual flow. The study further enhances
41 its novelty by accompanying an in-depth analysis of FDCs, incorporating a Mixed Gamma Distribution (MGD)
42 to model both fast and slow flow components. Uncovering the influence of climate, geology, and hydrological
43 processes on MGD parameters, the study provides an advanced understanding of flow duration curve shapes. A
44 key advancement is the integration of a comprehensive analysis of time scale decomposition, process
45 decomposition, and statistical analyses, offering an in-depth exploration of streamflow variability controls in
46 Peninsular India, contributing significantly to advancing our understanding of the complex interactions shaping
47 streamflow patterns in the region.

1 Introduction

49 The hydrologic functioning of catchment systems in any given region is coevolved with the long-term climatology
50 and landscape features present in the region through mutual interactions operating across multiple spatial and
51 temporal scales (Wagener et al., 2013). These interactions and long-term feedbacks impart variability to
52 hydrologic processes that are characteristic of the region of interest, including runoff generation and riverine
53 transport processes, thus influencing water availability and reliability to human populations that depend on the
54 streamflow. Understanding streamflow variability in time and space across river basins in the region is therefore
55 very important for water resource management (Deshpande et al., 2016; Sinha et al., 2018) and the prediction and
56 mitigation of floods (Kale et al., 1997). The frequency of high flows, low flows, or flows within specific ranges,
57 is essential for risk assessment of water management projects involving control of streamflow variability. Correct
58 portrayal of streamflow variability at the scale of catchments and river basins is therefore an indispensable
59 component in many hydrologic applications.

60 The focus of this paper is on the flow duration curve (FDC), which is a compact description of temporal
61 streamflow variability at the catchment scale. The FDC represents (daily) streamflow values plotted against the
62 proportion of time the given flow is exceeded or equalled (Smakhtin, 2001; Vogel & Fennessey, 1994). The
63 graphical form of the FDC embeds within it the governing hydrologic processes and dominant flow characteristics
64 throughout the range of recorded streamflows at the catchment scale (Botter et al., 2008). In this sense, the FDC
65 is also an important signature of a catchment's rainfall to runoff transformation (Ghotbi et al., 2020a; Vogel &
66 Fennessey, 1994). FDC thus typifies the old proverb, "one picture is worth a thousand words" with its potential
67 to encapsulate much of the relevant information of streamflow variability in a single plot (Vogel & Fennessey,
68 1995), and has been used in many hydrologic applications. Vogel and Fennessey (1994) provide a brief history of
69 the application of flow duration curves in hydrology. Applications of FDC include waste load allocation (Searcy,
70 1959), water quality management (Searcy, 1959; Rehana & Mujumdar, 2011, 2012), reservoir and sedimentation
71 studies (Vogel & Fennessey, 1995), low-flow and flood analyses (Smakhtin, 2001), assessment of environmental
72 flow requirements (Smakhtin and Anputhas, 2006), and water availability for hydropower (Basso & Botter, 2012).

73 Streamflow observed in rivers results from the complex interplay of various hydrological processes, including
74 runoff generation, overland and subsurface flow, and evaporation. These processes operate across multiple time
75 and space scales, responding to climatic inputs and interacting with heterogeneous landscape properties.
76 Deciphering the controls on streamflow variability and understanding their manifestation in the FDC shape pose

Streamflow observed in a river is the culmination of interacting hydrological processes of runoff generation, overland and subsurface flow and evaporation, operating at multiple time and space scales, in response to climatic inputs and their interactions with a range of landscape properties, all of which are highly heterogeneous. This makes it challenging to decipher the process controls on streamflow variability, and their manifestation in the shape of the FDC (Cheng et al., 2012; Ghotbi et al., 2020b; Yokoo & Sivapalan, 2011). Therefore, there is a need for appropriate conceptual frameworks that can bring out these process controls of FDCs and generate deep insights into the governing principles underpinning observed variability. Yokoo and Sivapalan (2011) presented a framework for deciphering the process controls of the FDC by considering the FDC of total streamflow (TFDC) as a statistical summation of a fast flow duration curve (FFDC) and a slow flow duration curve (SFDC). FFDC is a filtered version of precipitation variability, with rainfall intensity patterns and surface soil characteristics as controlling factors (Yokoo & Sivapalan, 2011). On the other hand, SFDC reflects a competition between subsurface drainage and evapotranspiration (Yokoo & Sivapalan, 2011), in which case seasonality and regional geology are stronger controlling factors. This contrast in the process controls governing quick (surface) runoff and slow (subsurface) flow, supports the notion of stratifying total streamflow into these two components operating at two different time scales. The distinction between the two (fast and slow) flow time scales enables the conceptualization of the process controls of fast flow (surface runoff) and slow flow (subsurface streamflow and groundwater flow) separately (Cheng et al., 2012; Yokoo & Sivapalan, 2011).

Ghotbi et al (2020a, 2020b) used this framework to explore the climatic and landscape controls of FDCs using streamflow data for hundreds of catchments across the continental United States in a comparative manner. In their work Ghotbi et al. (2020a) emphasized the need to consider the fast flow and slow flow time series independently as stochastic responses of catchments to sequences of storm events. Intensity and frequency of rainfall events and the properties of soils and topography govern the variability of fast flows, whereas climate seasonality and regional geology of the aquifer system govern variability of slow flow components. More specifically, Ghotbi et al. (2020b) showed the dominant process controls of FDCs as aridity index, topographic slope, coefficient of variation of daily precipitation, timing of rainfall, time interval between storms, snow fraction, and recession slope.

3

Stewart (2015) introduces the Bump and Rise Method (BRM), a novel baseflow separation technique calibrated with tracer data or optimization methods for accurate replication of tracer-determined baseflow shapes. The study challenges the conventional practice of solely relying on streamflow for recession analysis, contending that it can be misleading in understanding catchment storage reservoirs. The study also suggests for implementing baseflow separation before recession analysis as a means to gain fresh insights into water storage reservoirs and potentially resolve existing issues associated with recession analysis.

Significant advancements have been achieved in unraveling the process controls influencing flow duration curves. However, challenges persist in extending this knowledge to large spatial scales. To address this, Leong and Yokoo (2022) proposed an innovative approach, aiming to enhance the flexibility and adaptability of hydrological models by transforming the representation of the subsurface component. This involves the creation of a flexible structure composed of interconnected linear reservoirs, derived from a distinctive multiple hydrograph separation procedure, offering a comprehensive interpretation of dominant processes impacting FDC shapes and understand the number of distinct hydrological processes involved. In this study, we adopted the method proposed by Ghotbi et al. (2020) and (2021) as a foundational step to characterize fast and slow flow components, recognizing its inherent limitations stemming from its empirical and subjective nature.

~~Due to significant differences between fast and slow process controls, each may be used to explain streamflow variability independently. While recognizing the necessity to represent the hydrological processes across two distinct time scales, this paper aims to develop a process based understanding of how regional scale features impact streamflow variability across Peninsular India, using the flow duration curve (FDC) as a signature of this variability. For this purpose, an extension of this concept was made by including seasonal (timing) streamflow variability in a regional context. To isolate the effects of the drivers on the observed FDCs and to identify the controls of time and process scales on streamflow variability, a modeling framework is presented that comprises partitioning streamflow in multiple ways: seasons/months in the time domain, east-west/north-south directions in the space domain, fast/slow flows in the process domain. Streamflow data available from a large number of stream gauges within and between the major river basins across Peninsular India is employed for this purpose.~~ Botter et al. (2008) addressed river basin streamflow variability by presenting a seasonal probability distribution for daily streamflows using a stochastic soil moisture model. Extending this to the annual scale, the study establishes analytical expressions for long-term flow duration curves, linking them to annual minima distribution through key basin parameters, including climate, ecohydrology, and geomorphology. Muller et al. (2014) presents a process-based analytical expression for flow duration curves in seasonally dry climates, employing a stochastic model for wet season streamflow and a deterministic recession with stochastic initial conditions for the dry season. The approach disentangles inter- and intra-annual streamflow variations effectively. Durighetto et al. (2022) develops analytical expressions for flow duration curves and stream length duration curves (SLDC) to classify streamflow and active length regimes in temporary rivers. It identifies two streamflow regimes (persistent and erratic) and three active length regimes (ephemeral, perennial, and ephemeral de facto) based on dimensionless parameters linked to streamflow fluctuations and catchment discharge sensitivity. The proposed framework, validated in Italy and USA catchments, reveals a structural relationship between streamflow and active length regimes, offering a promising tool for analyzing discharge and river network length dynamics in temporary streams.

154 Our approach to understanding spatial patterns across Peninsular India builds upon the foundational concept of
155 timescale decomposition, as previously explored in studies such as Botter et al. (2008), Muller et al. (2014), and
156 Durighetto et al. (2022). The decomposition of timescales, while not novel in our study, serves as a fundamental
157 framework, aiding our analysis of spatial dynamics in the region.

158 ~~The scientific novelty and methodological advancement of the paper lie in two interconnected aspects, which have~~
159 ~~not been adopted in the literature to date: (i) the timescale partitioning framework is used to study the relative~~
160 ~~contributions of different seasons to the FDC (repeated for fast and slow flow components), exploring how the~~
161 ~~relative contributions holistically vary across the whole region and using the framework to reconstruct the annual~~
162 ~~flow duration curve using seasonal flow duration curves, (ii) the Wegenerian approach in connecting the spatial~~
163 ~~variability of streamflow at a regional scale using flow duration curve. Thus, the main goal of this paper is to~~
164 ~~reconstruct the flow duration curves at different scales to unravel the regional scale streamflow variability by~~
165 ~~extending the process partitioning (Ghotbi et al., 2020a) with the time partitioning. Studies that use simultaneous~~
166 ~~partitioning of flow duration curves at seasonal and process scales to investigate regional streamflow variability~~
167 ~~in space and seasonal climatic in time fluctuations using the Wegenerian approach are limited.~~ The novelty of the
168 paper lies in exploring the controls of streamflow variability in Peninsular India, a result of the impacts of
169 monsoons – southwest (summer season) and northeast (winter season), the presence of western and eastern ghats,
170 and topographical gradients. The paper advances the field by partitioning streamflow into three distinct time-wise
171 categories (non-monsoon, southwest monsoon, and northeast monsoon) and two process-wise partitions (fast flow
172 and slow flow), using flow duration curves as a tool. This approach allows for a detailed examination of the
173 relative contributions of each season and process to the overall annual flow.

174 Furthermore, the integration of a comprehensive approach to analysing flow duration curves by incorporating a
175 Mixed Gamma Distribution (MGD) to model both fast and slow flow components, along with seasonal and
176 regional exploration, enhances the study's novelty, and the study uncovers the influence of climate, geology, and
177 hydrological processes on MGD parameters, providing a better understanding of flow duration curve shapes. The
178 inclusion of links between MGD parameters and landscape properties, as well as the association between the
179 midsection slope of the FDC and recession parameters, adds an additional layer of sophistication to the analysis.
180 This provides a more robust understanding and offers insights into spatial variations, highlighting the integrated
181 role of surface and subsurface processes in shaping the catchment's average flow regime

182 The study stands out for its innovative combination of time scale decomposition, process decomposition, and
183 statistical analyses, offering a holistic exploration of the controls of streamflow variability in Peninsular India.
184 The partitioning approach and the integration of statistical analysis contribute significantly to advancing our
185 understanding of the complex interactions shaping streamflow patterns in this region. We recognize the abundance
186 of literature in FDC studies, but we believe our contribution is valuable in providing a detailed understanding of
187 the controls on streamflow variability in the context of Peninsular India.

188 Leong and Yokoo~~Leong et al.~~ (2022) introduced an innovative approach, employing interconnected linear
189 reservoirs to enhance hydrological model flexibility and adaptability. Carlier et al. (2018) addressed the neglect
190 of geological characteristics in catchment studies, revealing that climate conditions predominantly influence
191 medium to high discharge percentiles, while the catchment's ability to buffer meteorological forcing is attributed

to geological features. Botter et al. (2013) identified an index incorporating climate and landscape attributes to discriminate between erratic and persistent flow regimes, providing a robust framework for characterizing hydrology in the face of global change. Basso et al. (2015) investigated the role of non-linear storage–discharge relations in shaping high-flow distributions, emphasizing the importance of analyzing individual events for accurate characterization. Ye et al. (2012) explored regional variations in streamflow regime behavior across the U.S., highlighting the significance of snowmelt, vegetation cover dynamics, and climate trends. Fenicia et al. (2014) linked perceptual hydrological models with mathematical structures, demonstrating how distinct catchment processes influence model performance and emphasizing the need to synthesize experimentalist and modeler perspectives. Together, these studies contribute to a comprehensive understanding of FDCs and advance our knowledge of hydrological processes at different scales.

While the existing literature, represented by studies such as Leong and Yokoo~~Leong et al.~~ (2022), Carlier et al. (2018), Botter et al. (2013), Basso et al. (2015), Ye et al. (2012), and Fenicia et al. (2014), has made significant strides in understanding the controls of flow duration curves and streamflow variability, our study distinguishes itself by focusing on the unique hydrological context of Peninsular India. The previously discussed works have primarily addressed FDC drivers at regional or global scales, examining factors such as hydrogeology, climate, and landscape alterations. In contrast, our study delves into the specific challenges posed by the Peninsular Indian environment, characterized by the interplay of monsoons, mountainous terrain, and topographical gradients. Through a comprehensive approach encompassing time scale decomposition and process decomposition, and statistical analyses, we employ FDC as a key tool to unravel the controls of streamflow variability across Peninsular India. Our work enhances the understanding of hydrological processes in a region with distinct monsoonal influences, thus advancing the state of the art and providing valuable insights for water resource management in Peninsular India.

The remainder of the paper is structured as follows. Section 2 elaborates on the details of the study area and the daily streamflow dataset used. The description of the ~~conceptual framework~~methodology employed for the analysis is presented in Section 3. The results of the application of the framework to Peninsular India and the interpretation of the results are presented in Sections 4 and 5, respectively. Finally, the paper is concluded in Section 6 with key insights gained for the nature and controls of streamflow variability across Peninsular India.

2 Study region

Peninsular India is a cratonic region with an approximate shape of a vast inverted triangle with diverse topography and characteristic climatic patterns, bounded by the Arabian Sea in the west, the Bay of Bengal in the east, and the Vindhya and Satpura ranges in the north. The long escarpments of the Western Ghats and the Eastern Ghats, constituting the western and eastern continental fringes of India, and an asymmetric relief with eastward tilt towards the floodplains of several eastward draining rivers from the 1.5 km high Western Ghats, characterize the physiography of Peninsular India (Richards et al., 2016).

The rise of the Himalayan-Tibetan plateau has significantly contributed to the Neogene climate of Asia, favoured the birth of the modern monsoon (Fig. 1.a, b) (Chatterjee et al., 2013, 2017), and triggered glaciation in the Northern region. A wide variety of plateaux, open valleys, bedrock gorges, mountain ranges, inselbergs and residual hills constitute the geomorphology of Peninsular India (Kale & Vaidyanadhan, 2014). The Peninsular

landscape is dominated by Deccan Traps (Deccan basalts) of Cretaceous-Eocene, igneous and metamorphic rocks (Granite-gneisses) of Archaean-Late Precambrian along with minor consolidated sediments (Sandstone, shale) of Precambrian-Jurassic (Fig. 1.c) (Kale, 2014).

The region is strongly impacted by monsoons, major seasonal winds which are a manifestation of the seasonal movement of the Intertropical Convergence Zone (ICTZ in Fig. 1.a and Fig. 1.b), which contribute largely to the annual rainfall variability in much of the Indian subcontinent (Gadgil, 2003). The monsoons have two components – South-West monsoon and North-East monsoon, which arrive during June – September (JJAS) and October – December (OND), respectively. South-West monsoon season contributes more than 75% of annual rainfall over majority of the regions of the country (Saha et al., 1979). However, the Southern Peninsula receives a significant portion (30-60%) of its annual rainfall during the North-East monsoon, which contributes only 11% of the rainfall annually to India as a whole (Rajeevan et al., 2012). The maximum extent of rainfall over the Southern Peninsula during the North-East Monsoon is due to the reversal of lower-level winds over South Asia from the South-West to the North-East during the retreating phase of the South-West monsoon (Rajeevan et al., 2012). ~~In Peninsular India, there is a spatial variability of the South West monsoon in the south north direction. For example, the Western Ghats, located at the western edges of Krishna and Cauvery basins, obstruct the incoming South-West monsoon winds causing heavy rainfall on the mountains. After crossing the Western Ghats, the monsoon winds have less moisture, causing a sharp decline in rainfall amounts towards the central and the north-eastern part of the Peninsula (Fig S2.a in Supplementary Material). The North-East monsoon occurs during winter, and mostly influence the rainfall in the Cauvery and some parts of the Krishna basins.~~ Peninsular India displays south-to-north variability in the South-West monsoon, causing heavy rainfall along the Western Ghats and reduced amounts in the central and northeastern regions (Fig S2.a in Supplementary Material).

~~Vegetation on the long escarpment of Western Ghats is primarily tropical evergreen forest, which plays an important role in intercepting the South-West monsoon winds (Ramachandra, 2018). Ramachandra (2018) portrayed the profile of vegetation across the west-east gradient as it varies from tropical-evergreen to semi-evergreen and then moist to dry deciduous forests towards the rain-shadow region just east of the Western Ghats.~~ The Western Ghats' long escarpment hosts predominantly tropical evergreen forest, crucial for intercepting South-West monsoon winds (Ramachandra, 2018). Ramachandra (2018) depicted a west-east vegetation gradient along the Western Ghats, transitioning from tropical-evergreen to semi-evergreen and progressing to moist to dry deciduous forests towards the rain-shadow region in the east. The topography map for the Peninsular region and a selected point in the region is depicted in Fig. S1.a and Fig. S1.b in Supplementary Material, respectively. ~~The western margin of Peninsular India experiences heavy rainfall due to the presence of Western Ghats, whereas the rain shadow region witnesses deficient rainfall (Fig. S2.c). It can thus be seen that the long geological, tectonic history and the onset of monsoon climate events have made an imprint in the shaping the present landform of the Indian Peninsula (Kale, 2014).~~ The western margin of Peninsular India, influenced by the Western Ghats, receives heavy rainfall, while the rain shadow region experiences deficient rainfall (Fig. S2.c). The geological and tectonic history, coupled with monsoon climate events, has significantly shaped the present landform (Kale, 2014).

The region shown in Fig. 2 is selected as the study area in the Deccan Plateau of Peninsular India. The escarpment of Western Ghats forms the western margin of the Deccan Plateau which serves as the main water divide for the

268 Peninsular River systems. The gentle slope from west to east causes Peninsular rivers such as the Mahanadi,
269 Godavari, Krishna, and Cauvery (Fig. 2) to flow eastwards. Three of these rivers (Godavari, Krishna and Cauvery)
270 originate from the Western Ghats, spread across the area from the Deccan Plateau, flow eastwards, and drain into
271 the Bay of Bengal. The Mahanadi River rises in the mountains of Siwaha bounded by the Eastern Ghats in the
272 south and east, and drain eastwards into the Bay of Bengal. Additional details about the river basins can be found
273 in Text T1 within the Supplementary Information. The study utilizes daily streamflow data (1965-2012) from 62
274 gauges across four river basins, sourced from the Water Resources Information System (WRIS) database. Analysis
275 incorporates a daily gridded rainfall product ($0.25° \times 0.25°$) from the India Meteorological Department (Pai et al.,
276 2014).

277
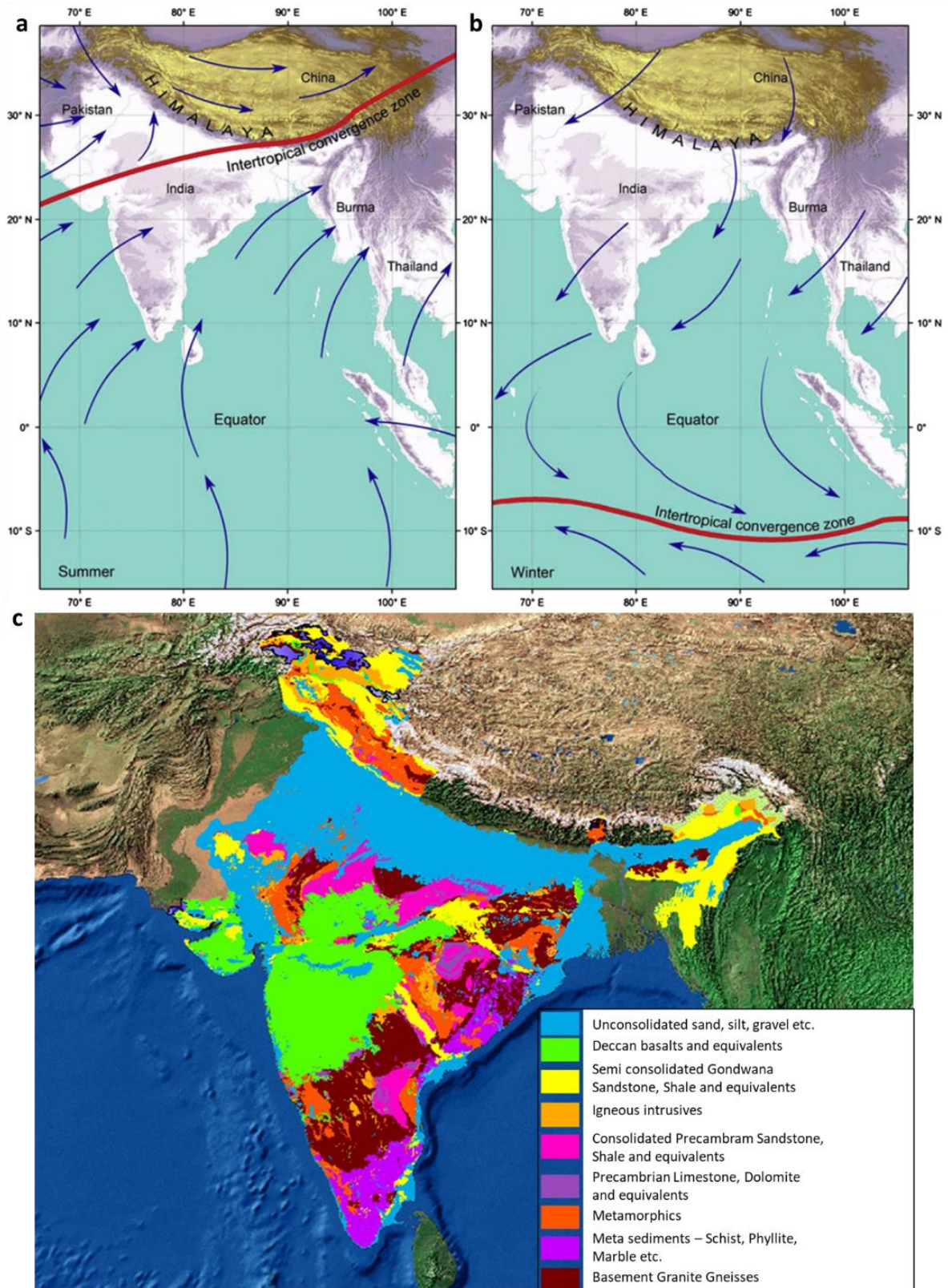
Figure 1. (a) The relation of uplift of Himalaya-Tibetan Plateau and monsoon initiation in India. Monsoon winds blow from the Indian Ocean towards land in the summer (b) during the winter, the Himalaya prevents cold air from passing into the subcontinent and causes the reversal of wind direction and monsoon blow from land toward sea [Reprinted from (Chatterjee et al., 2013)] (c) geology of Peninsular India [Reprinted from: Central Ground Water Board(https://www.aims-cgwb.org/general-background.php)].

9

The region shown in Fig. 2 is selected as the study area in the Deccan Plateau of Peninsular India. The escarpment of Western Ghats forms the western margin of the Deccan Plateau which serves as the main water divide for the Peninsular River systems. The gentle slope from west to east causes Peninsular rivers such as the Mahanadi, Godavari, Krishna, and Cauvery (Fig. 2) to flow eastwards. Three of these rivers (Godavari, Krishna and Cauvery) originate from the Western Ghats, spread across the area from the Deccan Plateau, flow eastwards, and drain into the Bay of Bengal. The Mahanadi River rises in the mountains of Siwaha bounded by the Eastern Ghats in the south and east, and drain eastwards into the Bay of Bengal. The Mahanadi basin constitutes a total catchment area of about 141,600 km^2 with an average annual rainfall of 1,360 mm and a mean annual river flow of 66,640 million m^3 (Rao et al., 2017). With an annual average rainfall of 1096 mm, the Godavari, the largest of all Peninsular rivers, receives nearly 84 percent of its annual rainfall on average during the South West monsoon (Koneti et al., 2018). The Godavari basin's challenges include frequent flooding in its deltaic lower reaches, given the area's proximity to the coastal zone, which is prone to cyclones, and frequent drying up during the drier months (Koneti et al., 2018). Krishna is Peninsular India's second largest river, with a total catchment area of 2,60,000 km^2, and is susceptible to floods and droughts in some specific regions (Chanapathi & Thatikonda, 2020). The South West monsoon is the most significant contributor to rainfall in the Krishna basin, accounting for about 90% of its total rainfall; the Krishna Basin, however, has a non-uniform rainfall distribution caused by climate variability, with an average annual rainfall bout of 770 mm (Chanapathi & Thatikonda, 2020). Annual rainfall in the Cauvery varies from 621 mm in the lower reaches to 4137 mm in the mountainous uplands, exhibiting considerable variation across the basin (Kumar Raju & Nandagiri, 2017). The river Krishna, with a mean annual runoff of less than 100 mm, is designated as an arid river (Milliman JD, 2011; Gupta et al., 2022), Cauvery as a semiarid river (100-250 mm), Mahanadi and Godavari as humid rivers (250-750 mm). The higher baseflow index occurs within 0.5 and 0.7 in catchments in the Godavari and Mahanadi basins, whereas the lower baseflow index is noted from 0.25 and 0.45 in the Cauvery and Krishna basins(Bhardwaj et al., 2020). For agricultural purposes, the semiarid regions of the Cauvery basin rely more on groundwater than surface water when compared to the other three basins (Sreelash et al., 2020).

In this study, daily streamflow data between 1965 to 2012 for 62 stream gauges (Fig. 2) are selected from Water Resources Information System database (WRIS) and located across the four river basins. The daily gridded rainfall product at spatial resolution of 0.25° × 0.25° from India Meteorological Department (IMD) is also employed for the analysis (Pai et al., 2014).

314

315
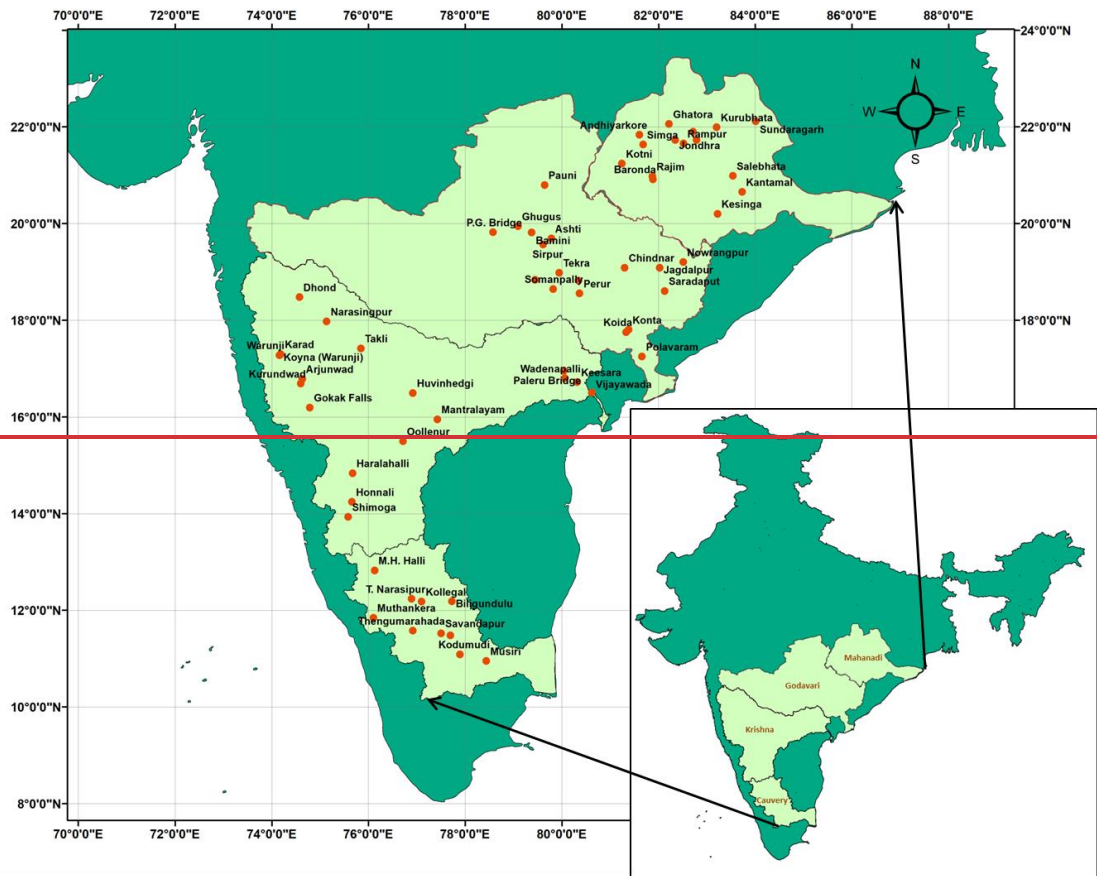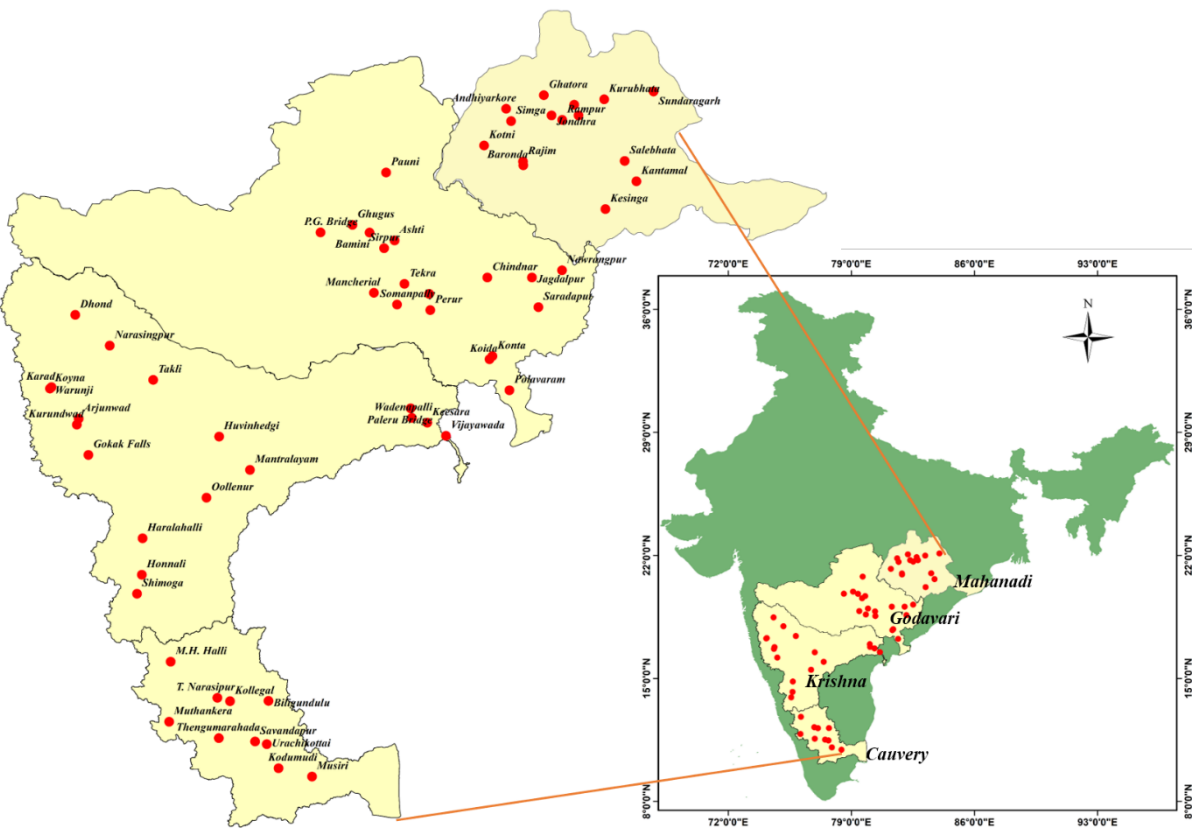
Figure 2. Location map of four Peninsular River Basins. Stream gauges considered in this study are marked with red circles.

318

3 Methodology

Initially, the study employs time scale partitioning to analyze flow duration curves across Peninsular India, focusing on Non-monsoon, South-West monsoon, and North-East monsoon periods in four river basins. The analysis extends to regional scales, encompassing streamflow time series from all gauging stations, and includes process scale partitioning to assess the relative contributions of fast and slow flow components, revealing spatial patterns influenced by climate, geology, and aquifer characteristics.

Additionally, the methodology entails a comprehensive analysis of FDCs for fast and slow flow components across seasons. It includes scaling time series to remove the influence of mean climate and geology, utilizing the statistical distributions to examine parameters influencing FDC shapes. The study explores links between statistical parameters and landscape properties through recession analysis and investigates spatial variation in FDC parameters using descriptors such as latitude, longitude, and catchment area. The final part of the methodology focuses the association between the midsection slope of the FDC and recession parameters, exploring the role of both surface and subsurface processes in controlling the average flow regime of the catchment.

In this section, we check the suitability of a framework to stratify observed streamflow time series in the time domain into distinct time scales to better understand the physical controls of streamflow variability across the region. Partitioning of streamflow across seasonal and monthly time scales is able to bring out the role of climate seasonality on streamflow variability. Moreover, the progression of the seasons spatially imparts signatures on streamflow variability regionally as a whole. Time scale partitioning thus offers an opportunity to understand these climatic and landscape controls on streamflow variability through quantifying the relative contributions of seasonal streamflow on annual streamflow variability and how they vary regionally.

The streamflow hydrograph is the response of a physical, deterministic system (catchment) to a sequence of rainfall events. Given that the rainfall events are very much random in all their properties, equivalently, the streamflow hydrograph can also be seen as a stochastic time series, with streamflow considered a random variable. Therefore, it is amenable to a stochastic treatment in terms of distribution functions (e.g., cumulative distribution function, CDF). A major advantage of the CDF is that it enables us to make a concise statement of streamflow variability across a population of events. They have diagnostic value in that they can explain or interpret a catchment's streamflow response and compare it across many catchments and they help to classify catchments based on the flow regimes. They also have practical value in engineering design and environmental monitoring that require a probabilistic treatment of streamflow. The cumulative distribution function of a random variable

3.1 *Time Scale Partitioning*

360 The streamflow hydrograph, representing a catchment's response to random rainfall events, is treated as a
361 stochastic time series, with streamflow considered a random variable. Utilizing distribution functions like the
362 cumulative distribution function (CDF) allows for a concise assessment of streamflow variability, aiding in the
363 interpretation and comparison of catchment responses. CDFs have diagnostic and practical value, facilitating the
364 classification of catchments based on flow regimes and supporting probabilistic treatments in engineering design
365 and environmental monitoring. The cumulative distribution function of a random variable (the random variable
366 of interest to us is daily streamflow; *Q*) expresses the probability that a realization (i.e., observation) of *Q* does
367 not exceed a specific value *q*.

368 The flow duration curve, an equivalent measure of streamflow variability, represents the fraction of time (D) that
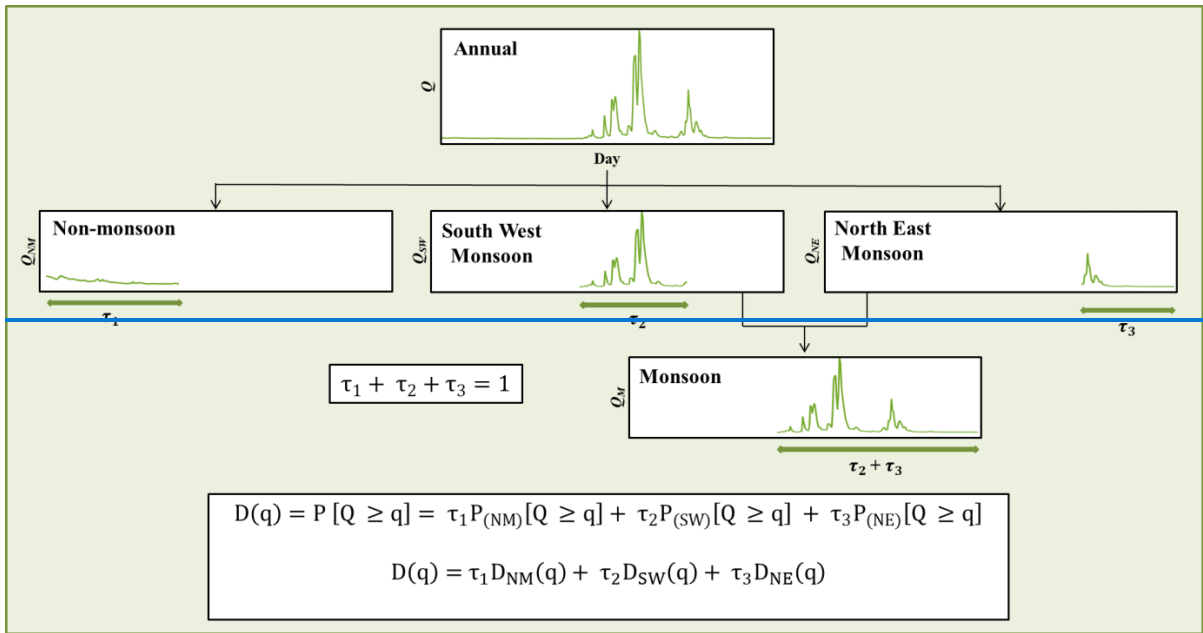369 streamflow is likely to equal or exceed a specified value, expressed mathematically as,

$$D(q) = P[Q \geq q] = 1 - F(q) \tag{1}$$

370 Despite its probabilistic definition, the flow duration curve is commonly plotted in hydrological applications as
371 q(D), i.e., *q* (in the vertical axis) as a function of *D* (in the horizontal axis).

372 The streamflow time series can be equivalently divided into temporal segments of distinct seasons as well as
373 distinct months. In this case, by joining observed time series over multiple years, FDCs for each time segment can
374 be reconstructed. Assuming independence (as an approximation), these can then be combined to generate annual
375 FDCs. The theory for the time scale partitioning is illustrated in Fig. 3a. The year is divided into three distinct
376 (non-overlapping) seasons, viz. Non-monsoon, South-West, and North-East seasons (for Peninsular India) of

13

relative durations τ_1, τ_2, and τ_3 (with $\tau_1 + \tau_2 + \tau_3 = 1$) respectively. These seasons can be assumed to have distinct characteristics in terms of rainfall variability and how they translate to streamflow variability. The daily streamflow time series is used to construct the seasonal as well as annual FDCs. For example, the FDC of Non-monsoon season is constructed by using the daily streamflow during the period of January – May over the years. Similarly, FDCs for South-West and North-East monsoons are constructed using the daily streamflow during June – September and October – December months over the years respectively and the annual FDC is constructed using daily streamflow values for 365/366 days over the years. The FDCs at monthly time scales are obtained using the daily values of streamflow in a month over the years. The FDCs for the three distinct seasons, i.e., Non-monsoon, South-West monsoon, North-East monsoon, are denoted as $D_{NM}(q)$, $D_{SW}(q)$, and $D_{NE}(q)$ respectively. Initially, the FDCs for each season can be constructed separately (Fig. 3a).

Annual

Q

Day

Q_{NM} Non-monsoon

Q_{SW} South West Monsoon

Q_{NE} North East Monsoon

τ_1

τ_2

τ_3

$\tau_1 + \tau_2 + \tau_3 = 1$

Q_M Monsoon

$\tau_2 + \tau_3$

$$D(q) = P\,[Q \geq q] = \tau_1 P_{(NM)}[Q \geq q] + \tau_2 P_{(SW)}[Q \geq q] + \tau_3 P_{(NE)}[Q \geq q]$$

$$D(q) = \tau_1 D_{NM}(q) + \tau_2 D_{SW}(q) + \tau_3 D_{NE}(q)$$

a

Annual

Q

Day

Q_{NM} Non-monsoon

Q_{SW} South West Monsoon

Q_{NE} North East Monsoon

τ_1

τ_2

τ_3

$\tau_1 + \tau_2 + \tau_3 = 1$

Q_M Monsoon

$\tau_2 + \tau_3$

b

Q

Day

Fast flow

Slow flow

Q_f

Q_s

Day

Day

$Q = Q_f + Q_s$
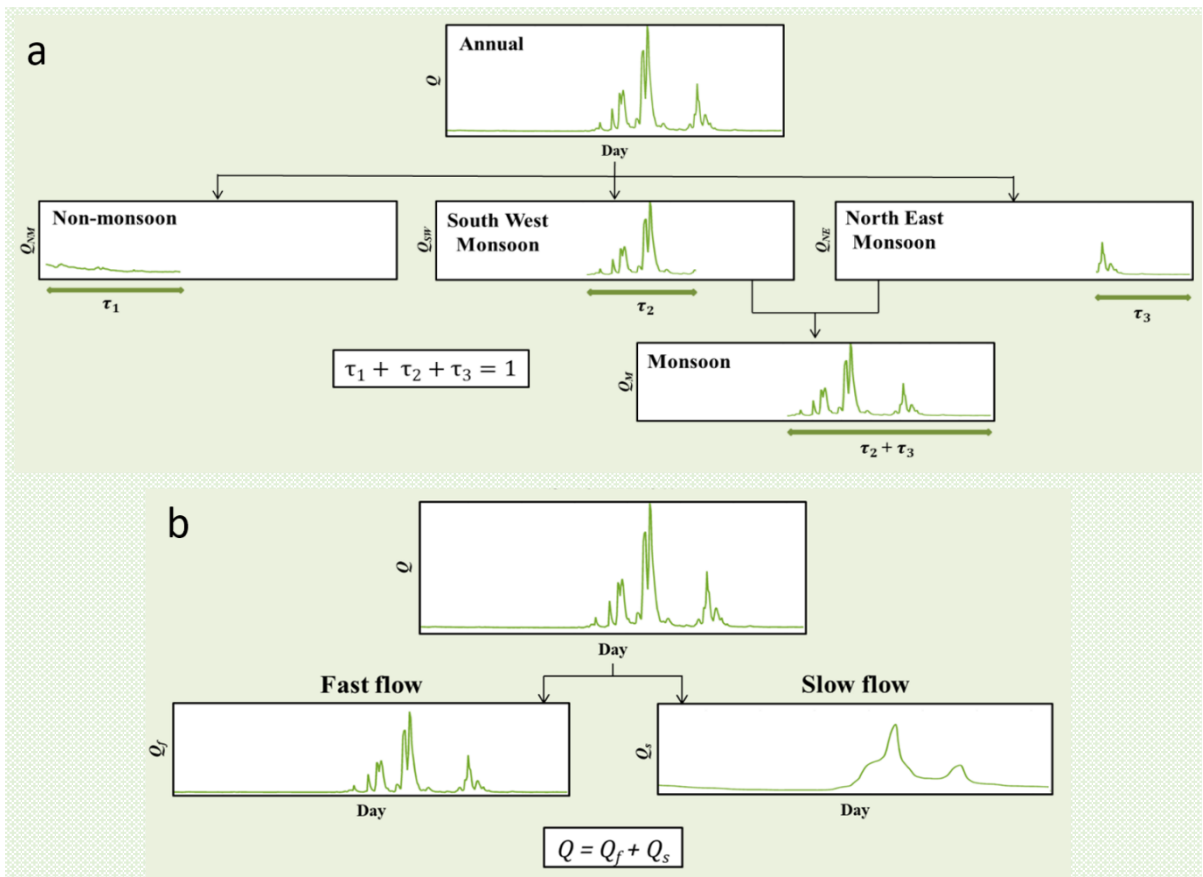
Figure 3a. Scale partitioning into seasonal and monthly time scales. The conceptual framework illustrates the time scale partitioning of streamflow time series into various seasonal components considering patterns of rainfall variability. The annual streamflow time series is decomposed into three components: (1) Non-monsoon flow, (2)

392 South-West monsoon flow, and (3) North-East monsoon flow. **Figure 3b.** The schematic representation illustrates

393 the process partitioning of streamflow time series into the fast flow and slow flow components.

394

395

396

397 The annual FDC with exceedance probability $P[Q \geq q]$ refers to the probability of flow in annual scale being

398 greater than or equal to q, and is expressed as

$$D(q) = P[Q \geq q] = \tau_1 P_{(NM)}[Q \geq q] + \tau_2 P_{(SW)}[Q \geq q] + \tau_3 P_{(NE)}[Q \geq q] \tag{23}$$

or, $\quad D(q) = \tau_1 D_{NM}(q) + \tau_2 D_{SW}(q) + \tau_3 D_{NE}(q)$ (34)

399 where, $P_{(NM)}[Q \geq q]$, $P_{(SW)}[Q \geq q]$ and $P_{(NE)}[Q \geq q]$ refer to, respectively, the probability of flow in Non-

400 monsoon, South-West monsoon and North-East monsoon being greater than q. As the seasons are non-

16

401 overlapping, the probability of flow being greater than q at annual scale (i.e., $P[Q \geq q]$) can be expressed as the
402 sum of the weighted probabilities of flow being greater than q in the three seasons.

403 In general, the FDC at the annual scale can be constructed as follows:

$$D(q) = \tau_1 D_1(q) + \tau_2 D_2(q) + \cdots + \tau_n D_n(q) \tag{45}$$

404 where n is the number of distinct seasons considered for the analysis and, $\tau_1 + \tau_2 + \cdots + \tau_n = 1$. The validity of
405 the above depends on the assumption that there is no carryover of flows from one season to the next season (which
406 is an approximation). In this study, the assumption of independence between flows across three seasons is checked
407 using multivariate Hoeffding's test (see details in Text T2S1 of Supplementary Information).

408 If $F_A(.), F_{NM}(.), F_{SW}(.)$ and $F_{NE}(.)$ represent cumulative distribution function of daily flows during annual, Non-
409 monsoon, South-West monsoon and North-East monsoon, respectively, then using equation (2), equation (6) can
410 be written as:

$$1 - F_A(q) = \tau_1[1 - F_{NM}(q)] + \tau_2[1 - F_{SW}(q)] + \tau_3[1 - F_{NE}(q)] \tag{6}$$

411 Differentiating the above equation with respect to q,

$$f_A(q) = \tau_1 f_{NM}(q) + \tau_2 f_{SW}(q) + \tau_3 f_{NE}(q) \tag{7}$$

412 where $f_A(.), f_{NM}(.), f_{SW}(.)$ and $f_{NE}(.)$ represent probability density functions of annual, Non-monsoon, South-
413 West monsoon and North-East monsoon flows respectively.

414 If Q, Q_{NM}, Q_{SW} and Q_{NE} represent random variables comprising of daily streamflow at annual, Non-monsoon,
415 South-West monsoon and North-East monsoon time scales respectively, the expectation $E(Q)$ and variance $V(Q)$
416 of annual flow in terms of seasonal flows can be expressed as

$$E(Q) = \tau_1 E(Q_{NM}) + \tau_2 E(Q_{SW}) + \tau_3 E(Q_{NE}) \tag{8}$$

$$V(Q) = \tau_1 E(Q_{NM}^2) + \tau_2 E(Q_{SW}^2) + \tau_3 E(Q_{NE}^2) - \left(E(Q)\right)^2 \tag{9}$$

417 The magnitudes of τ_1, τ_2 and τ_3 are $\frac{5}{12}, \frac{4}{12}$ and $\frac{3}{12}$ based on the annual proportions of Non-monsoon, South-West
418 monsoon and North-East monsoon respectively.

419 The same concept can be continued by combining the flows in different months, in which case the way to combine
420 monthly FDCs into an annual FDC is given by:

17

$$D(q) = \frac{1}{12} \sum_{m=1}^{12} D_m(q) \tag{10}$$

421 where $m = 1, \dots, 12.$

422 If Q_m represents the random variable daily streamflow over mth month, then the expectation $E(Q)$ and variance
423 $V(Q)$ of annual flow in terms of monthly flows can be expressed as

$$E(Q) = \frac{1}{12} \sum_{m=1}^{12} E(Q_m) \tag{11}$$

$$V(Q) = \frac{1}{12} \sum_{m=1}^{12} E(Q_m^2) - \left(E(Q_A)\right)^2 \tag{12}$$

424 The relative contributions of Non-monsoon ($C_{NM \to AN}$), South-West monsoon ($C_{SW \to AN}$) and North-East monsoon
425 ($C_{NE \to AN}$) flows to annual flow can be approximated through following expressions:

$$C_{NM \to AN} = \frac{\tau_1 E(Q_{NM})}{\tau_1 E(Q_{NM}) + \tau_2 E(Q_{SW}) + \tau_3 E(Q_{NE})} \tag{5\,13}$$

$$C_{SW \to AN} = \frac{\tau_2 E(Q_{SW})}{\tau_1 E(Q_{NM}) + \tau_2 E(Q_{SW}) + \tau_3 E(Q_{NE})} \tag{6\,14}$$

$$C_{NE \to AN} = \frac{\tau_3 E(Q_{NE})}{\tau_1 E(Q_{NM}) + \tau_2 E(Q_{SW}) + \tau_3 E(Q_{NE})} \tag{7\,15}$$

426 Similarly, the relative contributions of monthly flows to annual flow can be expressed as:

$$C_{m \to AN} = \frac{\frac{1}{12} E(Q_m)}{\frac{1}{12} \sum_{m=1}^{12} E(Q_m)} \tag{8\,16}$$

427 where, $m = 1, 2, \dots, 12$, represents the index for months.

428 Note, as before, these relative contributions to total flow effectively also measure the relative contributions of the
429 seasonal/monthly flows to the mean of the annual flow duration curve.
430 The methodology for constructing annual FDC using seasonal FDC is as follows:

431 1. The empirical PDFs – $f_{NM}(q), f_{SW}(q)$ and $f_{NE}(q)$ are derived for daily streamflow time series for Non-
432 monsoon, South-West monsoon and North-East monsoon seasons respectively.

433   2. These PDFs are then multiplied by scaling factors, $\tau_1, \tau_2 \text{ and } \tau_3$ in equation S49. The scaling factors represent

434   relative durations of the three seasons considered. For example, $\tau_1 = 5/12$, as the duration of duration of non-

435   monsoon season is 5 months.

436   3. The PDF of annual flow is estimated as the weighted sum of three scaled density functions corresponding to

437   three seasons (see Eq. S27). The annual flow consists of the daily streamflow for Non-monsoon, South-West

438   monsoon and North-East monsoon seasons.

439   The performance of the time scale partitioning framework is assessed using the metric, root mean square error

440   (RMSE). The method of estimation of q_{sim} is shown in Fig. S3.

441    $$RMSE = \sqrt{\frac{1}{n}\sum_{i=1}^{n}(q_{actual} - q_{sim})^2} \tag{917}$$

442

443   **3.2 Process Partitioning**

444   Daily streamflow is partitioned in such a way that it approximates the statistical summation of fast flow and slow

445   flow at the daily scale (Fig.3b):

$$Q = Q_f + Q_s \tag{10}$$

446   where Q is the daily streamflow, Q_f is the daily fast flow, Q_s is the daily slow flow.

447   The relative contributions of fast flow ($C_{\to TF}$) and slow flow ($C_{SF \to TF}$) to total flow can be expressed as

$$C_{Q_f \to Q} = \frac{Total\ Fast\ Flow\ Volume}{Total\ Flow\ Volume} \tag{11}$$

$$C_{Q_s \to Q} = \frac{Total\ Slow\ Flow\ Volume}{Total\ Flow\ Volume} \tag{12}$$

448   Note that $C_{Q_f \to Q}$ and $C_{Q_s \to Q}$ effectively measure the relative contributions of fast and slow flows to the mean of

449   the annual flow duration curve.

450   **3.3 Exploring Controls and Spatial Patterns of Flow Duration Curves: Insights from Statistical Distributions**

451   **and Analysis of Mid-Section Slope**

452   The analysis then extends to the comprehensive analysis of flow duration curves for fast and slow flow

453   components across different seasons, with a focus on understanding their variations and controls. The first step is

454   to scale the fast and slow flow time series by their respective long-term mean values, effectively removing the

455   influence of mean climate and geology. This scaling allows the identification of secondary controls on the shapes

456   of FDCs.

457   The Mixed Gamma Distribution (MGD) is then used to fit the scaled fast and slow flow time series, and the

458   parameters of the MGD are examined for their influence on the FDC shapes (see text T4 of Supplementary

459   Information) Krasovskaia et al., 2006; Botter et al., 2007; Muller and Thompson 2016; Santos et al., 2018. The

variation of the parameters of the MGD are explored, regionally and seasonally, considering the influence of mean climate, geology, and complex hydrological processes on fast and slow flows. The performance of the MGD in fitting FDCs is assessed using goodness-of-fit metrics such as the Nash-Sutcliffe efficiency (NSE) and coefficient of determination (R^2). Seasonal variations of MGD parameters are analyzed at a regional scale, considering all gauging stations. The study further explores the link between MGD parameters and landscape properties through recession analysis. The studies by Botter et al. (2013), Muller et al. (2014), Basso et al. (2015), Arai et al. (2021), Leong and Yokoo (2022; 2019) collectively enhance understanding of the intricate relationship between recession parameters and FDC characteristics. They emphasize the significant influence of recession parameters on hydrological regimes, catchment-scale attributes, non-linear storage-discharge relations, and the practical applications in predicting FDCs, showcasing a comprehensive exploration of the pivotal role these parameters play in shaping hydrological responses at various spatial scales. Leong and Yokoo~~Leong et al.'s~~ (2022) innovative modeling of subsurface components further contributes to a deeper comprehension of the dominant processes influencing FDC shapes. Spatial variation in FDC parameters is then investigated using descriptors such as latitude, longitude, and catchment area.

The final aspect of the methodology involves the association between the midsection slope of the FDC and recession parameters, emphasizing the role of both surface and subsurface processes in controlling the average flow regime of the catchment. The methodology aims to unravel the intricate interplay of climate, geology, and hydrological processes in shaping the regional hydrologic signatures of Peninsular India.

4 Results and Discussions
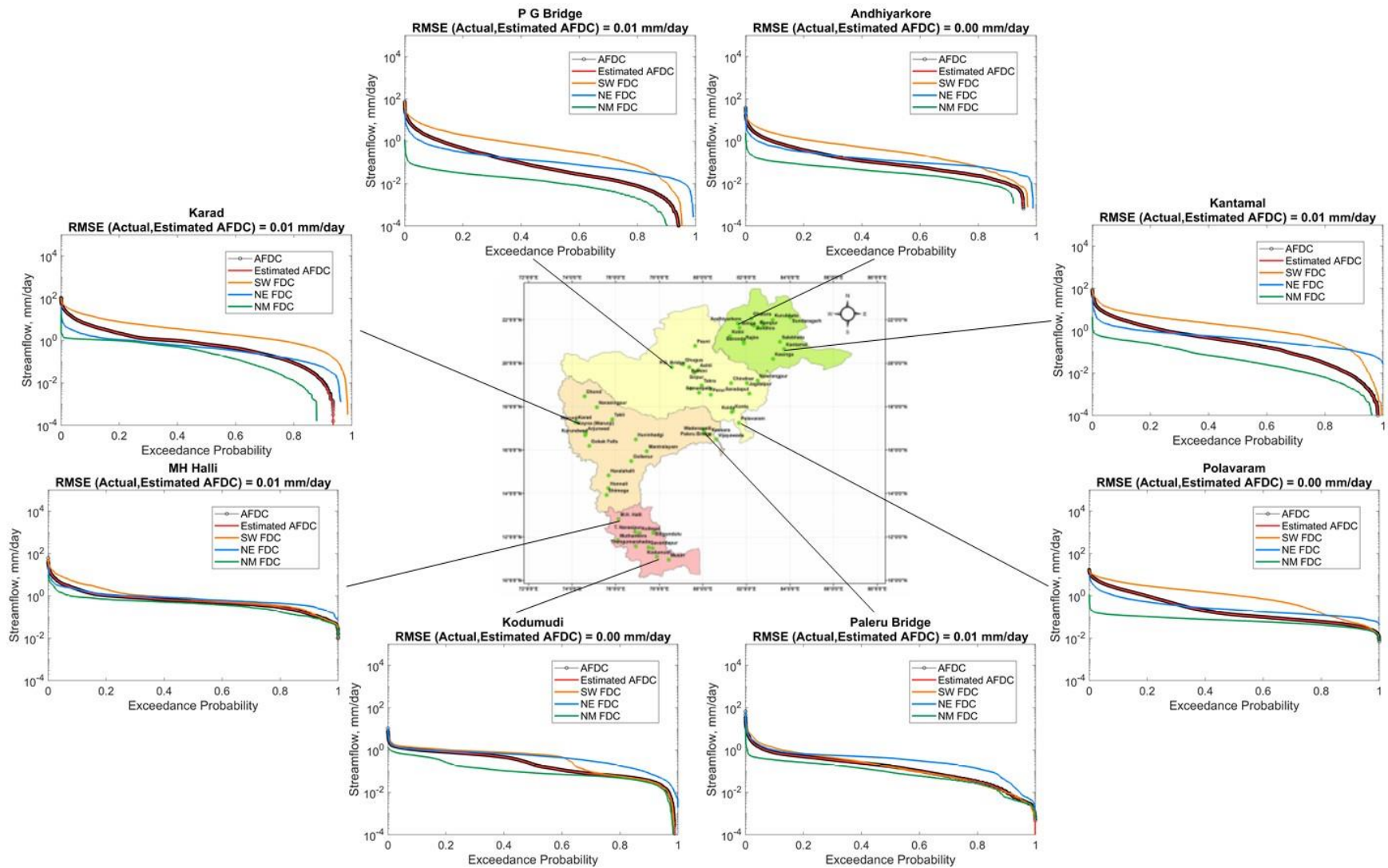
4.1 Time scale partitioning

We initially investigated the spatial variations in seasonal and annual flow duration curves across Peninsular India employing the partitioning framework. The annual flow duration curve and seasonal flow duration curves for Non-monsoon, South-West monsoon, and North-East monsoon are shown in Fig. 4 for eight representative gauges, one at the upstream and one at the downstream of each of the four river basins. The estimated annual flow duration curve (red curve) using ~~the~~ equation S2~~7~~ is also shown in Fig. 4. Daily streamflow time series is normalized by catchment area before plotting (on a semi-log paper) the flow duration curve for comparison across the gauging stations. In particular, the annual flow duration curve (black scatter) is reproduced well by the partitioning of both seasonal (red curve in Fig. 4) and monthly flows (red curve in Fig. S4). The mean and variance of annual flows are also reproduced well by the time scale partitioning framework (Fig. S5). This confirms the efficacy of the time scale partitioning approach of seasonal/monthly flows in approximating the annual flow duration curve (see also Fig. S4, Fig. S5.a and Fig. S5.d in Supplementary Material).

Another feature that can be observed in Fig. 4 is that in gauging stations located in the northern part of the peninsular region, flow duration curves (FDCs) of South-West monsoon flows (orange curve) are relatively higher than other seasonal FDCs. Given the logarithmic scale used to plot ~~of~~ the flows, this dominance is significant. In

496 sites located in the southern part of the region, the dominance of South-West monsoon is not as strong and North-

497 East monsoon flows (blue curve) are also significant.

498 Motivated by these observations, we extracted seasonal and monthly streamflow time series from the entire dataset

499 across all gauging stations to compute the relative contributions of seasonal and monthly flows to the annual flow

500 duration curve. The results are presented in Fig. 5. At the monthly scale (top panel, Fig. 5), the contributions of

501 flows during the months of June to September are much higher than in other months in northern Peninsular basins

502 (Mahanadi and Godavari, Krishna to a less extent). This can be explained by the contribution of monthly rainfall

503 to annual rainfall, which is higher during these months as shown in Fig. S6. On the other hand, in the southernmost

504 Cauvery basin, the dominance of June to September months is relatively not as strong, and there is also a

505 significant contribution during the months of October to December, higher than in northern basins (Fig. 5.d). This

506 can be attributed to the slightly more equal dominance of both South-West (June - September) and North-East

507 (October – December) monsoons over the Cauvery basin (Fig. S6.d) than in the northern basins. This pattern is

508 also reflected at the seasonal scale (bottom panel, Fig. 5), with the contribution of South-West monsoon flow to

509 annual flow being slightly higher than that during the other seasons, and much higher in northern basins. However,

510 the contribution of South-West monsoon to annual flow decreases in southern basins, while the contribution of

511 North-East monsoon increases, as can be seen clearly in Fig. 5.h for the Cauvery basin. The contribution of Non-

512 monsoon to annual flow is also higher in southern basins relative to northern basins. This can be attributed to

513 carry over flows from winter rains during the North-East monsoon, which is more pronounced in the southern

514 part of the region.

21

Figure 4. Spatial variations in seasonal and annual flow duration curves across Peninsular India. The time scale partitioning framework of seasonal flows in approximating annual flow duration curves works reasonably well.
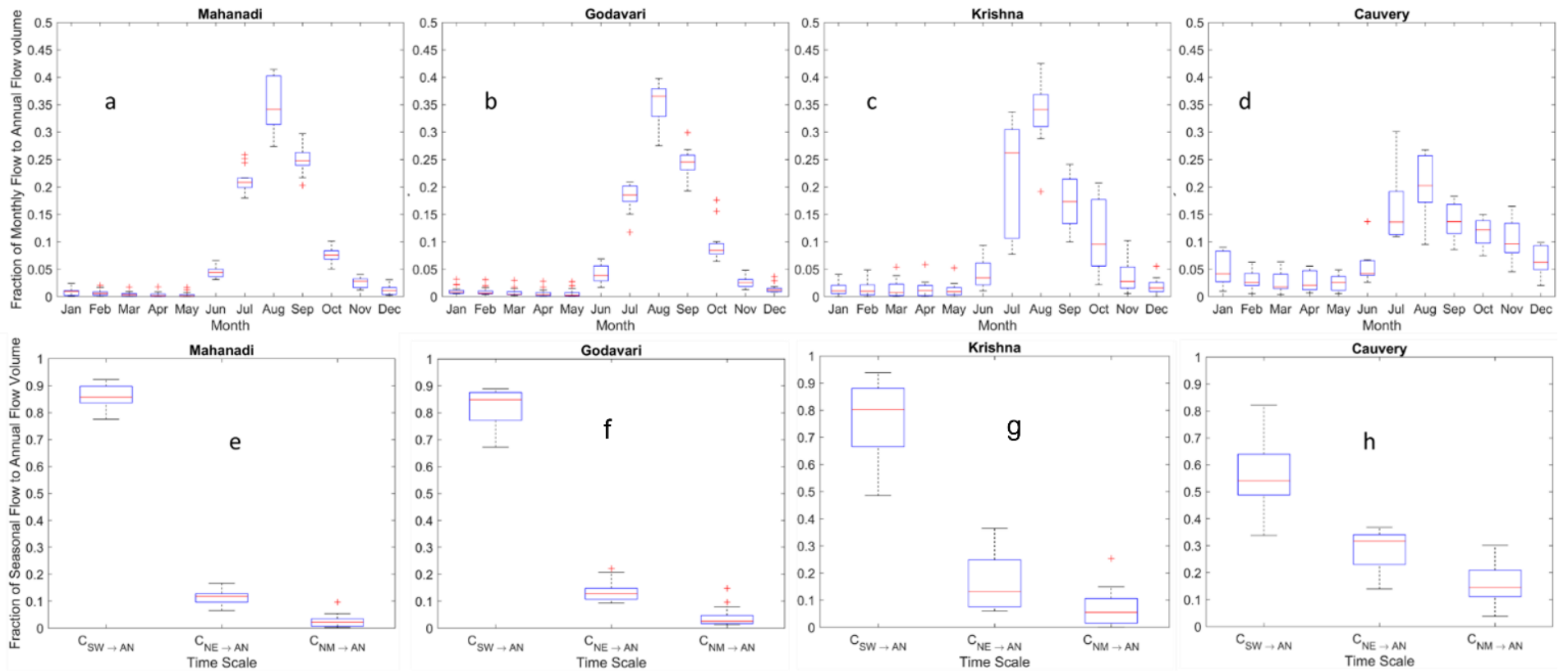
Figure 5. The relative contributions of monthly and seasonal flows to annual flow at basin scale. The contributions of South-West monsoon flow to annual flow increases in northern basins whereas it decreases in southern basins. However, the contributions of North-East monsoon flow to annual flow increases towards southern basins.
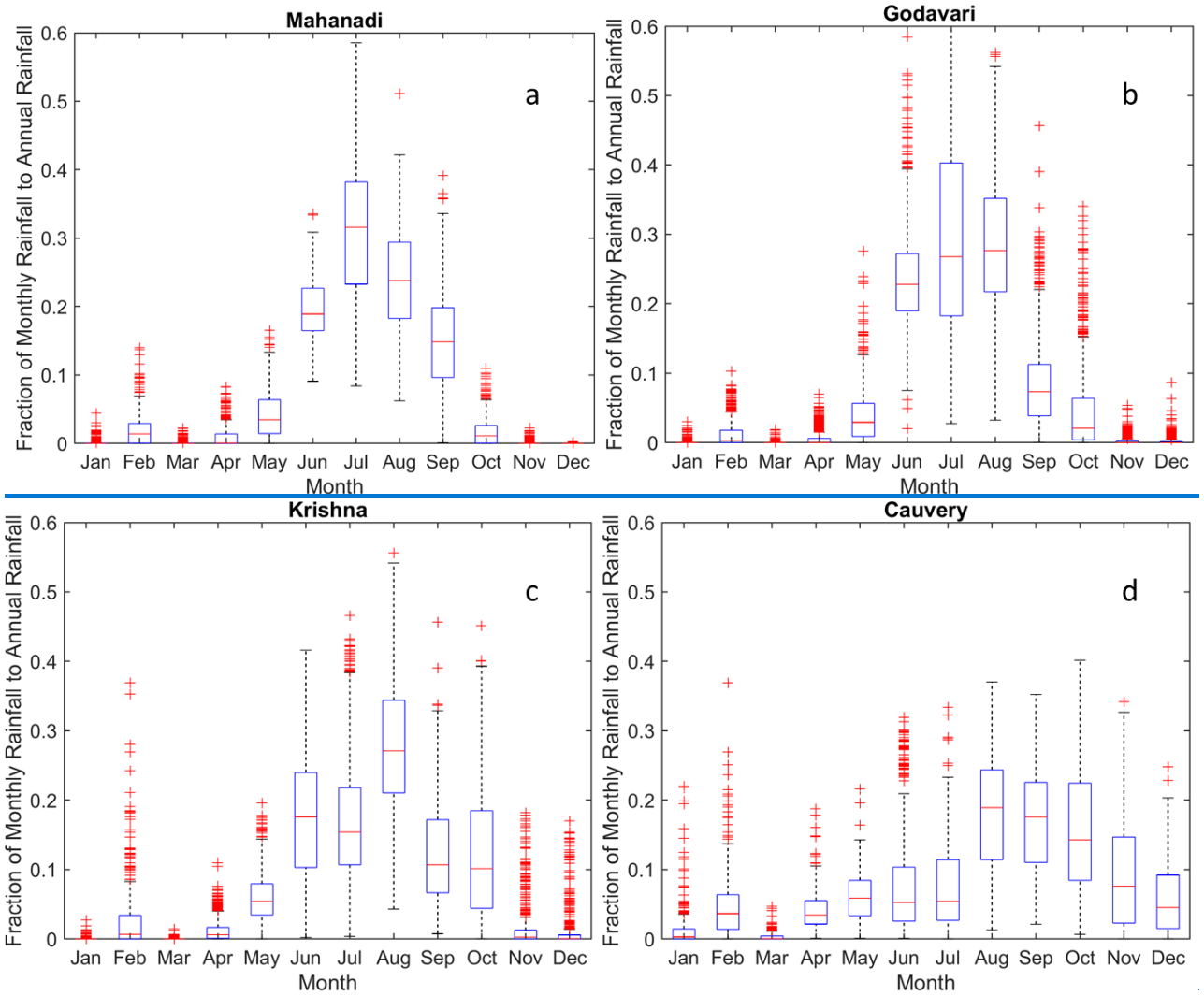
Figure 6. Long term (1951-2010) fractional contribution of monthly rainfall to annual rainfall across Peninsular basins.

24

524   We next carried out regional scale analysis by considering streamflow time series of all the gauging stations across
525   all four river basins. Similar to basin scale analysis presented before, the relative contributions of seasonal and
526   monthly flows to annual flow are now estimated at the regional scale (Fig. 67). The spatial patterns of South-West
527   and North-East monsoon rainfall across the Peninsular region are plotted for comparison using IMD gridded
528   rainfall product (Fig. 67.b and Fig. 67.e).

529   The contribution of South-West monsoon flows to annual flow increases in the northerly direction (Fig. 67.a).
530   The mountainous region of the southern Peninsula (western part of Krishna basin and north-western part of
531   Cauvery basin) receives high rainfall during the South-West monsoon season (Fig. 67.b – extended till 17° N
532   latitude). The streamflow produced in the headwater regions of southern basins in response to high rainfall,
533   contributes at least 70% of the annual flow (Fig. 67.a). Yet, the areal fraction of these high rainfall, headwater
534   regions within the four river basins is quite small and their contributions to the average precipitation or flow at
535   the basin scale is much smaller. There is also considerable variability in the contributions of South-West monsoon
536   flows to annual flow in the sub-basins located at the eastern and south-eastern parts of Krishna and Cauvery basins
537   (represented by the scatter below the regression line till 17° N latitude in Fig. 67.a) due to declining rainfall (Fig.
538   67c). This considerable variability, on average, reduces the overall contributions of South-West monsoon to
539   annual flow in southern Peninsula with respect to the basins in the northern part.

540   The northern part of the Peninsular region receives comparatively higher rainfall than the southern part without
541   considering the Western Ghats. This increased rainfall is attributed to the movement of low-pressure systems that
542   develop over the Bay of Bengal towards central India (Krishnamurthy & Ajayamohan, 2010; Prakash et al., 2015).
543   The low-pressure systems are a regular feature of South-West monsoon, which brings significant amount of
544   rainfall in the northern part of the Peninsular region (Krishnamurthy & Ajayamohan, 2010). The increased rainfall
545   (Fig. 67.b – after 16° N latitude) is responsible for higher contribution of South-West monsoon flows to annual
546   flow in the northern basins. As the spatial variability of this rainfall is comparatively less than in the southern
547   Peninsular region, there is less variability in the contribution of South-West monsoon flows to annual flow. The
548   spatial variability in South-West monsoon along the south-north direction across Peninsular region can explain
549   the gradient in the contribution of South-West monsoon flows to annual flow in the same direction.

550   On the other hand, the contribution of North-East monsoon flows to annual flow increases in the southerly
551   direction (Fig. 67.d and Fig. 67.e). This can be explained by the fact that the southern part of the Peninsular region
552   receives higher rainfall during North-East monsoon than the rest of the Peninsular region (Fig. 67.f).
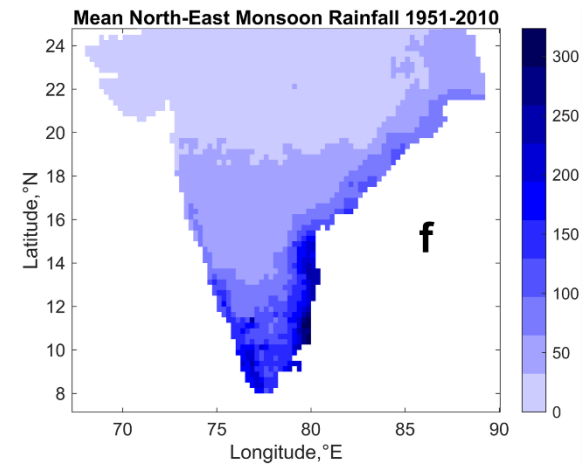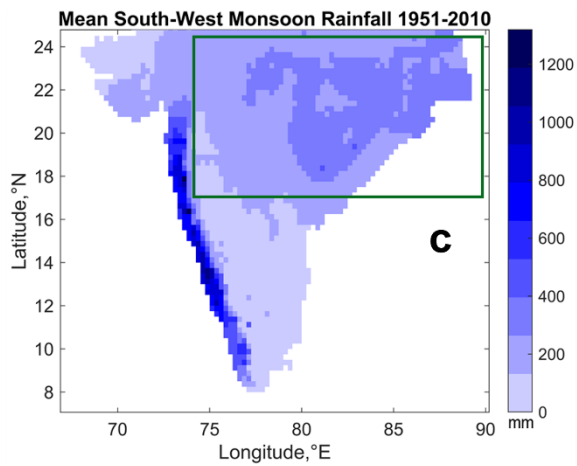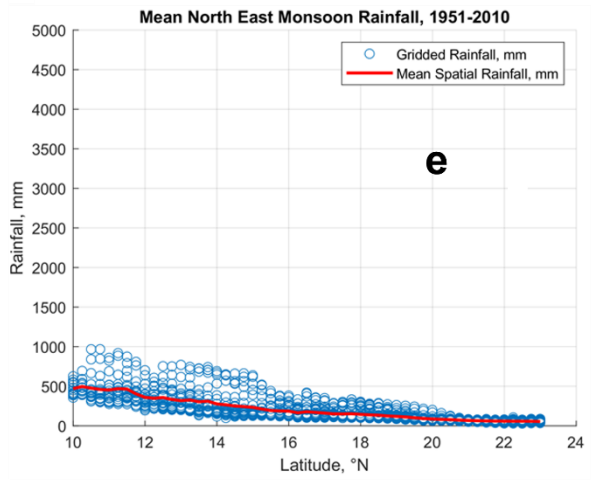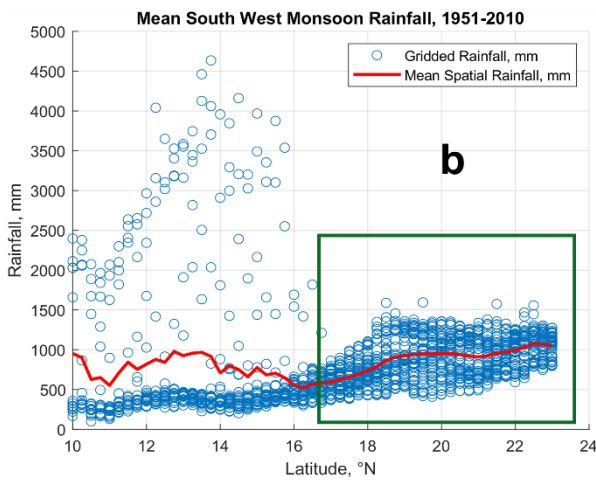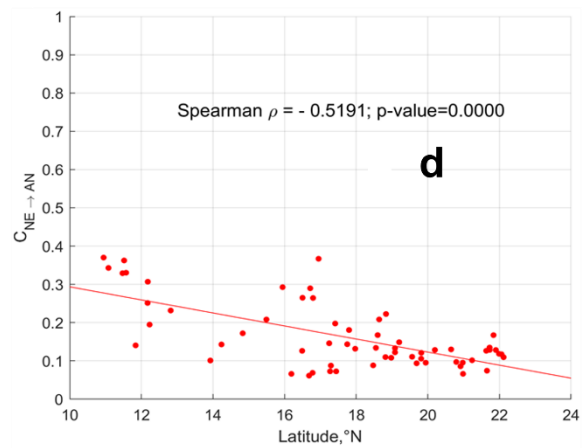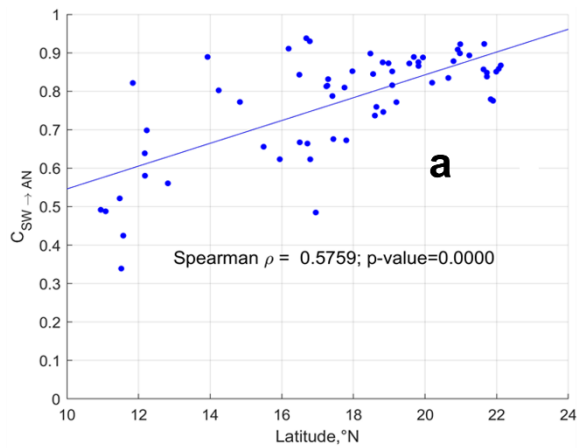
Figure 67. Contribution of seasonal flows to annual flow at regional scale. The spatial variability of South-West and North-East monsoons can explain the variation in contributions of seasonal flows to annual flow across south-north gradient. The green box in (b) indicates the northern part of peninsular region which receives higher rainfall than the southern part. The green box in (c) indicates the spatial extent of the rainfall grids which was considered in figure (b). The red line in figure (b) indicates the mean rainfall – obtained by averaging the rainfall values at a specific latitude (°N).

The application of the analysis framework used here is based on the critical assumption of independence of flows between different seasons (months), which needs to be critically evaluated. Moisture carry-over across seasons is a confounding issue in the case of strongly seasonal catchments (i.e., exhibiting sharp transition from wet season to dry season in terms of rainfall climatology), specifically when the initial wetness condition at the onset of the dry season depends on the final wetness at the end of wet season and vice-versa. Although most of the rainfall (58-90%) is concentrated during South-West monsoon months (i.e., June – September, red bar in Fig. S7~~6~~) in Peninsular basins, more than 10% of the annual rainfall is received during North-East monsoon months (i.e., October – December, yellow bar for Cauvery and Krishna in Fig. S7~~6~~). In addition, more than 8% of annual rainfall occurs in non-monsoon season (i.e., January – May, blue bar in Fig. S7~~6~~. This highlights that rainfall received during non-monsoon and North-East monsoon seasons are comparable, and thus it is difficult to distinguish the rainfall climatology across these seasons. Therefore, it is challenging to declare these are catchments with seasonally dry climates. In order to justify our assumption in the reconstruction of annual FDC from seasonal flows, we have now conducted a multivariate Hoeffding test (Gaißer et al., 2010) to check the independence between three random variables representing Non-monsoon, South-West Monsoon and North-East Monsoon flows respectively. A value of test statistic – φ^2 – close to zero indicates independence between three random variables. It is observed that except for two stations in Krishna basin, 60 out of 62 stations show independence between flows across the seasons (Fig. S8~~7~~). This supports appropriateness of the assumption of no carry-over that had been used in this study to construct annual FDC based on seasonal FDCs.

4.2 Combined influence of time scale and process scale partitioning

In order to further explore the climatic and landscape controls of streamflow variability regionally, we next partition streamflow into fast and slow flow components, notionally representing surface runoff, and a combination of subsurface and groundwater flow respectively (Ghotbi et al., 2020a, b) ~~(see details in Text S2 and Fig. S8 in Supplementary Material)~~. Fast flow is controlled by event scale runoff generation processes and its variability is characterized by topography, land use, soil and rainfall characteristics. On the other hand, climate seasonality and geologic formations of the subsurface are primary controllers of slow flow variability (Ghotbi et al., 2020a, b). The slow flow component is extracted from observed streamflow by using a recursive digital filter (see details in ~~Appendix A.1~~Text T5 of Supplementary Information). The fast flow component is obtained by then subtracting the slow flow from observed streamflow. The relative contributions of fast flow and slow flow to total flow (and hence also mean annual flow) are estimated using equations ~~S2~~11 and ~~S3~~12 respectively, for all the gauging stations across all four basins. The relative contributions of fast and slow flows to total flow at the basin and regional scales (combining all the gauging stations) are shown in Fig. 7~~8~~. In addition, the long-term mean annual rainfall across the Peninsular region is also presented for comparison and to possibly explain the contributions of fast flow (Fig. 7~~8~~.h).

The contributions of fast and slow flows to total flow in each of the four river basins is presented in Fig. 7~~8~~.a to Fig. 7~~8~~.d, indicating a strong dominance of fast flow in the northern basins (close to 80% in Mahanadi, Godavari and Krishna), and relatively less dominance (around 60%) in the southern Cauvery basin. This dominance of fast flow also shows up at the regional scale (Fig. 7~~8~~.e). The regional variations of the relative contributions of slow and fast flows to total flow can also be seen in the results for individual gauges presented in Fig. 7~~8~~.f and Fig.

598   78.g, respectively. On average, the contribution of slow flow decreases in the northerly direction, while the
599   contribution of fast flow increases in a corresponding way.

600   The contribution of fast flow to total flow increases in the northern direction of the Peninsular region (Fig. 78.g).
601   The fast flow component of streamflow is generally more responsive to the characteristics of rainfall intensity.
602   The southern part of the region receives high rainfall over Western Ghats along the western edge of Krishna basin
603   and Cauvery basin (Fig. 78.h). In Cauvery basin, the headwater catchments (namely, MH Halli, Muthankera and
604   Thengumarahada in Fig. S6) contribute 57 – 65 % of fast flow to total flow locally. The subbasins located at the
605   western edges of Krishna basin contribute 80% of the fast flow to total flow (between 13° N and 18°N latitudes
606   in Fig. 78.g) locally. However, there is a wide range of variability in the contributions of fast flow to total flow
607   for subbasins located in the eastern part of Krishna basin. The spatial mean rainfall increases and variability
608   decreases after 16° N latitude (Fig. 78.h), which dictate the increased contribution fast flow to total flow.
609   Therefore, the spatial characteristics (mean and variability) of annual rainfall control the south-north gradient in
610   fast flow contributions to total flow. In order to explain the variability in slow flow fraction of total flow, a
611   multivariate regression analysis is performed (details are provided in ~~Appendix, A.5~~Text T8). It is observed that
612   the location of the gauges is an important predictor of the slow flow fraction of total flow in Peninsular region,
613   revealing the existence of regional groundwater gradient in the region (Table T~~A.~~1). In addition to the location of
614   the gauges, the recession parameter, β – that controls the aquifer geometry and water level elevation profile during
615   early and late stages of recession – is found to be significant in explaining the slow flow fraction of total flow
616   (Table T~~A.~~1).

617   The contributions of slow flow to total flow increases in the southerly direction over the Peninsular region (Fig.
618   78.f). This can be explained by two major factors. Firstly, the Peninsular region is mostly dominated by hard rock
619   geologic formations, where the subsurface flows are controlled by secondary porosities due to weathering and
620   fracturing (Chandra, 2018; Das, 2019). The distribution of these formations is highly heterogenous (Fig. 1.c) and
621   is responsible for baseflow (slow flow) contribution to total flow (Collins et al., 2020; Narasimhan, 2006). For
622   example, 84% of the total area of Cauvery basin is classified as moderate and good groundwater potential zone
623   (Arulbalaji et al., 2019). The influence of such potential regions of Cauvery basin is reflected on the presence of
624   significant amount of slow flow even in the Non-monsoon season (Fig. 89.g and Fig. 89.h). Likewise, 63% of the
625   total area of Krishna basin is classified under same category (Harini et al., 2018). However, the slow flow regime
626   becomes much more seasonal (Fig. 89) in the northern part of the Peninsular region due to limited capability of
627   geologic formations in transmitting slow flow (Patil et al., 2017) as well as strong seasonality in rainfall patterns
628   (Fig. 89). Secondly, the southern part of the Peninsula receives rainfall almost equally during both South-West
629   and North-East monsoons, which is reflected in the bimodal pattern of rainfall seasonality (Fig. 89.g and Fig.
630   89.h). The compounding effect of bimodal rainfall seasonality and higher fraction of moderate to good
631   groundwater potential zones explains the higher contribution of slow flow to total flow in southern part of the
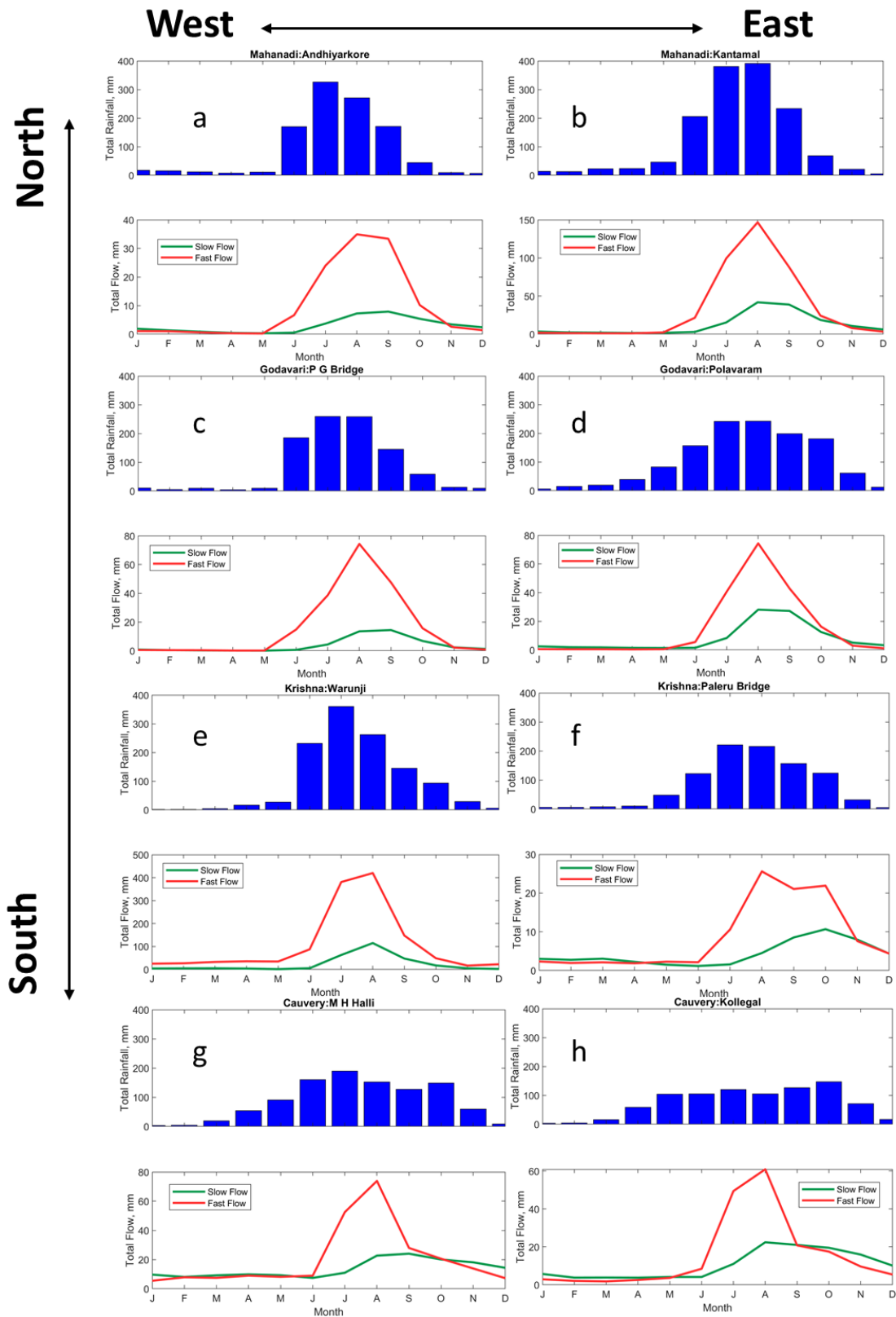632   Peninsular region.

633

634
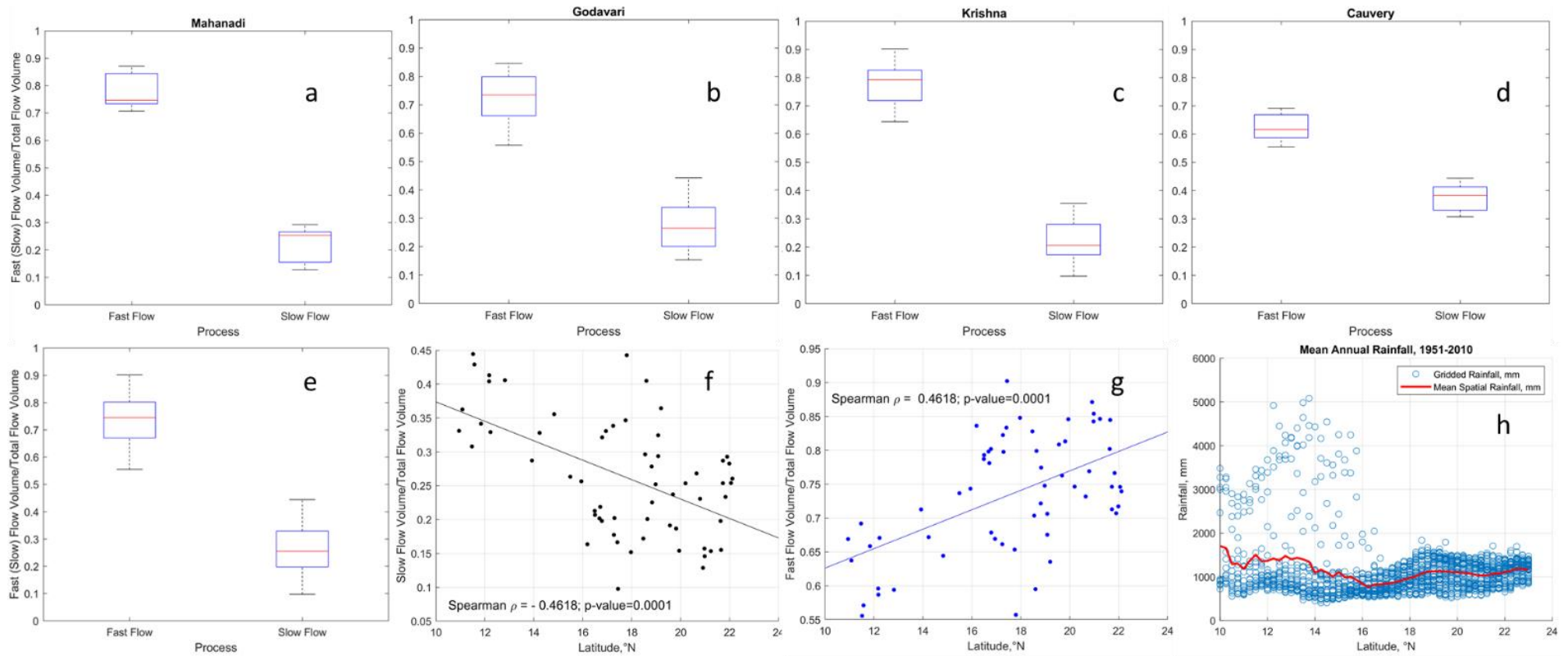
635

636 **Figure 78.** Relative contributions of fast and slow flow to total flow. Consistent higher contribution of fast flow and lower contribution of slow flow to total flow are observed
637 in Peninsular India (a – d) at basin scale. At regional scale, a systematic gradient in fast and slow flow contributions is observed (f and g). The spatial patterns of rainfall (h)
638 can explain the gradient in fast flow contributions. The high scatter of rainfall in the low latitudes represents the heavy rainfall with high variability occurring in the Western
639 Ghats.

Further, an investigation of the combined influence of climatic time scales and process time scales is therefore pertinent to fully understand the controls of streamflow variability in this region. To address this question, we extracted the fast and slow flow components for each of the Non-monsoon, South-West monsoon and North-East monsoon seasons. These components are then used to estimate their relative contributions to total flow for the three seasons across all the gauging stations.

The relative contributions of fast and slow flow to total flow at basin scale are shown in Fig. 9. It is observed that during the Non-monsoon period, the median contributions of fast and slow flow for Mahanadi, Krishna and Cauvery basins are similar, although there exists considerable variability in their distribution. With the onset of the South-West monsoon, the contribution of fast flow to total flow increases markedly for all the basins, although relatively much less in the Cauvery basin. During the subsequent North-East monsoon season, the contribution of fast flow decreases whereas slow flow contribution increases. The fluctuations in the fast flow contributions can be explained by the onset and withdrawal of the monsoon seasons, which are major contributors to fast flow generation. The fluctuations in the fast flow contributions across seasons can be explained by the differences in the rainfall amount during South-West and North-East monsoons (Fig. 6.c and Fig. 6.f). Among all four basins, the difference in median contributions of fast and slow flow is minimum. These can be attributed to the presence of higher fraction of moderate and good groundwater potential zones (Arulbalaji et al., 2019) which promotes baseflow even in dry periods (Fig. 8.g and Fig. 8.h). The presence of bimodal pattern in rainfall seasonality due to both South-West and North-East monsoons minimizes the difference between the relative contributions of fast and slow flow to total flow.

West ← → **East**

North ... **South**

Mahanadi:Andhiyarkore   a

Mahanadi:Kantamal   b

Godavari:P G Bridge   c

Godavari:Polavaram   d

Krishna:Warunji   e

Krishna:Paleru Bridge   f

Cauvery:M H Halli   g

Cauvery:Kollegal   h

Figure 89. Spatial variation of long-term monthly fast and slow flow components of streamflow at selected gauges in Peninsular region. The blue bar plots represent the long-term monthly rainfall averaged over the sub-basins corresponding to the gauging stations. The seasonality in rainfall patterns changes (unimodal to bimodal) across north-south direction of the Peninsular region.

659

660
661
662
663

31

664 Further, an investigation of the combined influence of climatic time scales and process time scales is therefore
665 pertinent to fully understand the controls of streamflow variability in this region. To address this question, we
666 extracted the fast and slow flow components for each of the Non-monsoon, South-West monsoon and North-East
667 monsoon seasons. These components are then used to estimate their relative contributions to total flow for the
668 three seasons across all the gauging stations.

669 The relative contributions of fast and slow flow to total flow at basin scale are shown in Fig. 10. It is observed
670 that during the Non-monsoon period, the median contributions of fast and slow flow for Mahanadi, Krishna and
671 Cauvery basins are similar, although there exists considerable variability in their distribution. With the onset of
672 the South-West monsoon, the contribution of fast flow to total flow increases markedly for all the basins, although
673 relatively much less in the Cauvery basin. During the subsequent North-East monsoon season, the contribution of
674 fast flow decreases whereas slow flow contribution increases. The fluctuations in the fast flow contributions can
675 be explained by the onset and withdrawal of the monsoon seasons, which are major contributors to fast flow
676 generation. The fluctuations in the fast flow contributions across seasons can be explained by the differences in
677 the rainfall amount during South-West and North-East monsoons (Fig. 7.c and Fig. 7.f). Among all four basins,
678 the difference in median contributions of fast and slow flow is minimum. These can be attributed to the presence
679 of higher fraction of moderate and good groundwater potential zones (Arulbalaji et al., 2019) which promotes
680 baseflow even in dry periods (Fig. 9.g and Fig. 9.h). The presence of bimodal pattern in rainfall seasonality due
681 to both South-West and North-East monsoons minimizes the difference between the relative contributions of fast
682 and slow flow to total flow.
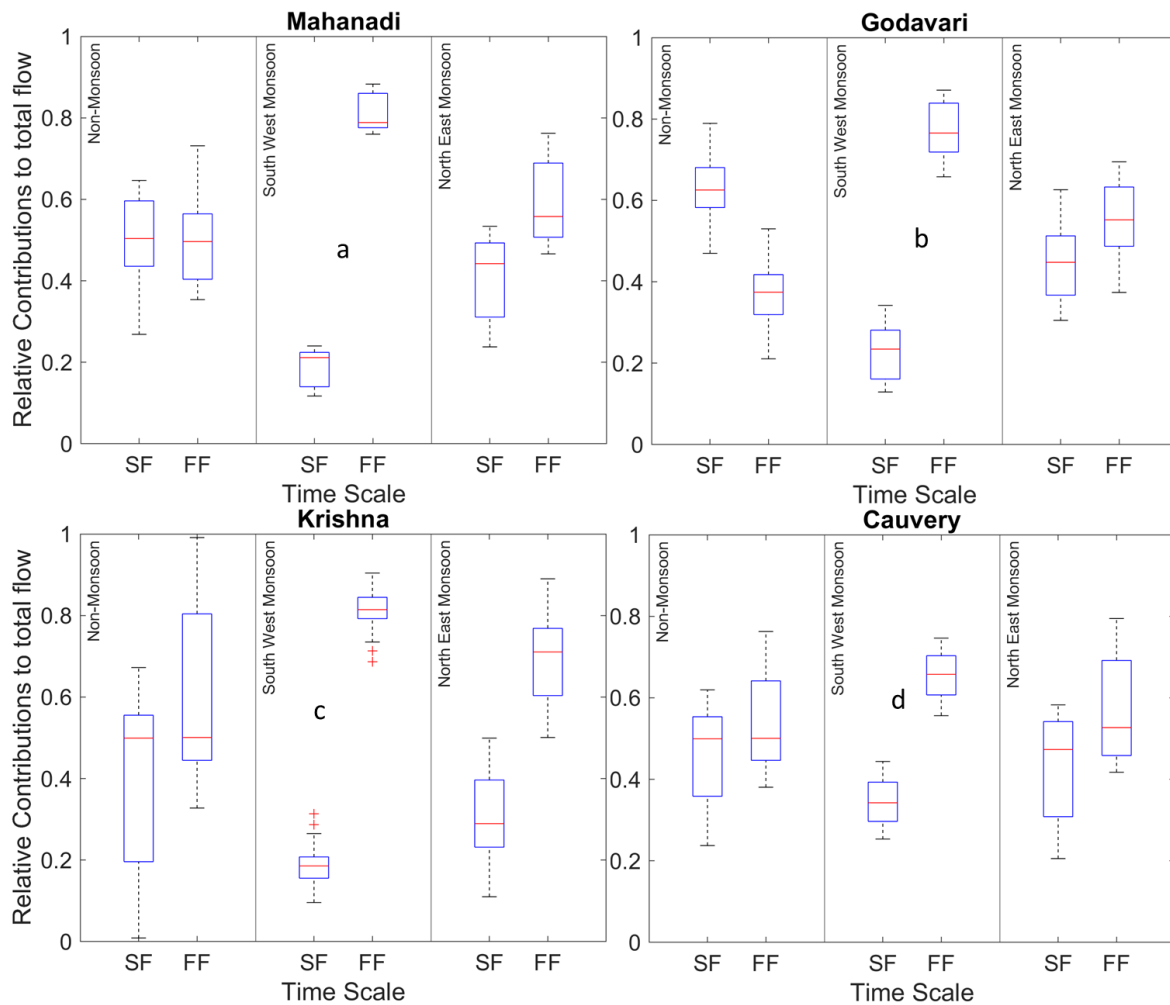
Figure 910. Seasonal contributions of fast (FF) and slow flow (SF) to total flow at basin scale.

5. Stratification of streamflow variability

5.1 Understanding physical controls and spatial variation of flow duration curve by fitting statistical distributions

So far in this paper, in order to understand the physical controls on regional streamflow variability across Peninsular India we have partitioned observed streamflows in two ways: (i) seasonal/monthly flows, and (ii) slow and fast flows. We looked at the relative contributions of these components to mean annual streamflow, looked at how the relative contributions varied regionally, and attributed these to the relative strengths of the monsoons and spatial variations of geological formations. We now return to the FDCs of the flow components, especially the shapes of the FDCs (as reflected in the parameters of the fitted distribution) and look at how they themselves vary regionally.

In our study the fast and slow flow time series are scaled by their respective long-term mean values to remove the influence of mean climate and geology, thus providing an opportunity to identify the secondary controls on the variation of shapes of FDCs. The scaled fast and slow flow time series are now used to fit the mixed gamma distribution (MGD, (see details in ~~Appendix A4~~Text T4 of Supplementary Information). The parameters of mixed

33

gamma distribution control the shape and orientation of the FDC. For example, the shape parameter k controls the slope of the FDC whereas α controls the zero-flow part of the FDC. However, the parameter θ affects the vertical shift of the FDC. In addition, these parameters are also linked with the mean and variance of the streamflow time series. For example, the scale parameter θ is directly proportional to the mean of the time series whereas, the shape parameter k is inversely proportional to the variance of the time series.

As the fast and slow flow time series are scaled with their respective long-term means, the scale parameter (θ) is approximately found to be inversely proportional to shape parameter (k) through the relationship, $k\theta = \frac{1}{1-\alpha}$ (Cheng et al., 2012). Therefore, the variations of only k and α – zero-flow probability, are presented in this section. The variation of k can be related to the steepness of the FDC, i.e., smaller values of k will have steeper slopes.

The Nash-Sutcliffe efficiency (NSE) and coefficient of determination (R^2) goodness of fit of fast/slow flows to MGD is shown in Fig. S10 (in Supplementary Information). In addition, the observed and simulated fast and slow flow FDCs are compared in Fig. S8 (in Supplementary Information). It is observed that the slow flow component fits well to mixed gamma distribution than fast flow component, as slow flow is most stable component and MGD satisfactorily captured the shape of slow flow FDC. However, MGD adequately captures the shape of fast flow FDCs at upper tail (high flow segment), except for the lower tail (low flow segment). The fast flow processes are governed by more complex processes (for example, infiltration and saturation excess runoff generation, runoff routing, stochastic nature of storm events, properties of soil and topography etc.) than slow flow (for example, climate seasonality and underlying geology of aquifer system).

The seasonal variation of parameters of the mixed gamma distribution at regional scale (comprising of all the gauging stations) is presented in Fig. 10. The mixed gamma distribution performed well in fitting the flow duration curves of two flow components across different seasons (Fig. S10). In Fig. 10.a, it is observed that the shape parameter of slow flow is consistently higher than that of fast flow. The shape parameter is inversely proportional to the variance of streamflow. The slow flow exhibits lower variance due to its longer time of residence in the subsurface formations. Moreover, the subsurface formations in Cauvery River basin are more favourable to slow flow in comparison to the other three basins (Fig. 8.g and Fig. 8.h). In addition, the bimodal seasonal pattern of rainfall is also responsible for occurrence of slow flow even in the Non-monsoon period for the southern basins (Fig. 8).

The fast flow component exhibits higher variance than the slow flow component. The median shape parameter of fast flow is highest during South-West monsoon season and lowest during North-East monsoon (Fig. 10.a). This can be explained by the lower variance of fast flow during South-West monsoon as the rainfall amount is higher during the season compared to the North-East monsoon (Fig. 6.c and Fig. 6.f). The dominance of both South-West and North-East monsoons in Cauvery basin results in lower variance of fast flow compared to the northern basins. The fast flow duration curves are steeper than the slow flow duration curves for all seasons, as the magnitudes of k for fast flow are smaller than that of slow flow (Fig. 10.a).
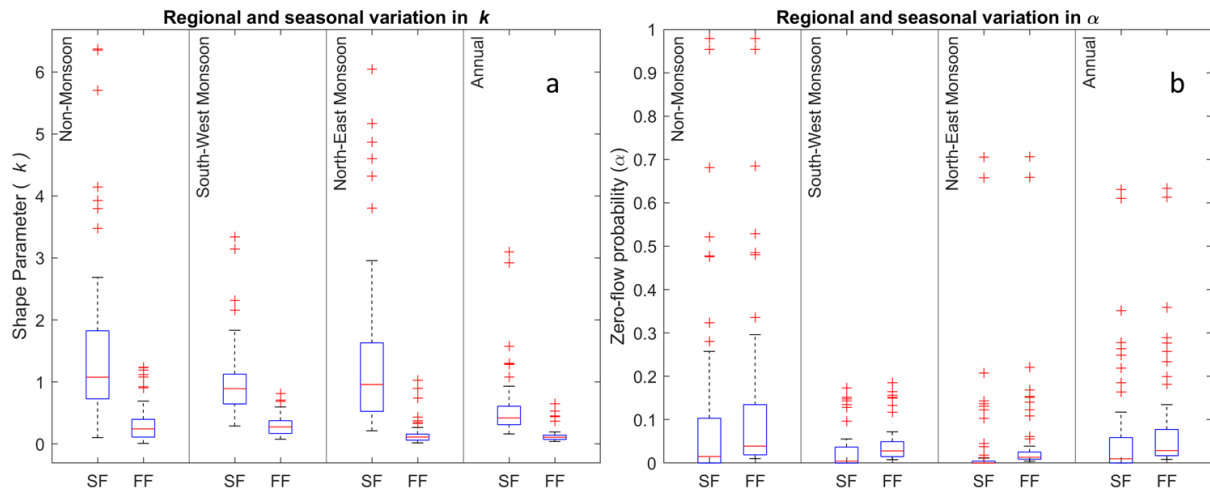
Figure 1~~1~~0. Regional and seasonal variation of k and α parameter of mixed gamma distribution.

~~The fast flow component exhibits higher variance than the slow flow component. The median shape parameter of fast flow is highest during South-West monsoon season and lowest during North-East monsoon (Fig. 11.a). This can be explained by the lower variance of fast flow during South-West monsoon as the rainfall amount is higher during the season compared to the North-East monsoon (Fig. 7.c and Fig. 7.f). The dominance of both South-West and North-East monsoons in Cauvery basin results in lower variance of fast flow compared to the northern basins. The fast flow duration curves are steeper than the slow flow duration curves for all seasons, as the magnitudes of k for fast flow are smaller than that of slow flow (Fig. 11.a).~~

The parameter α controls the zero-flow part of the flow duration curve. It is observed that the mean α for slow flow is minimum during South-West monsoon and maximum for Non-monsoon season (Fig. 1~~1~~0.b) on a regional scale. This can be attributed to the combined influence of rainfall during South-West monsoon and the connectivity between underlying geologic formations in the Peninsular region. For the fast flow, the mean α is minimum during the South-West monsoon and maximum during Non-monsoon as the South-West monsoon is the dominating rainfall season in Peninsular India.

The shape parameters (k) of MGD for slow and fast flow components are linked with landscape properties through recession analysis, where the parameters γ and β of power-law relationship are estimated using streamflow data (details in Text T6 in Supplementary Information~~Appendix A.2~~). It is observed that shape parameter (inversely proportional to variability) of slow flow is positively correlated with β. The parameter β is influenced by aquifer geometry and water table elevation profile defining early and late stages of recession (Tashie et al., 2020a; Tashie et al., 2020b). Higher values of β indicate slow late recessions which is characterized by low variability in slow flow (Fig. 1~~1~~2.a).

The shape parameter of fast flow is negatively correlated with the parameter γ of the power-law relationship (Fig. 1~~1~~2.b). The parameter γ strongly related with the seasonality of catchment wetness and evapotranspiration which are primary governing factors for runoff generation (Dralle et al., 2015; Gnann et al., 2021). In addition, the spatial

760 variation of rainfall also influences the variability of γ (Biswal & Kumar, 2014) which reflects the variability of
761 fast flow.

762 The variation of the parameters, k and α was also studied using spatial descriptors (latitude and longitude) as
763 explanatory variables to understand the spatial variation of FDCs across south-north, west-east gradients. In
764 addition, the behaviour of these parameters is also assessed using catchment area as another explanatory variable.
765 The regional parameter sets comprising of k and α are next constructed for slow and fast flow processes by
766 including these parameters for all the time series across different gauging stations across the Peninsular region.
767 The Spearman correlation coefficients between these parameters and explanatory variables (i.e., catchment area
768 and spatial descriptors – latitude and longitude) for slow and fast flow processes at seasonal scales are computed.
769 The schematic representation of significant directions (positive/negative correlations) in Spearman coefficient is
770 shown in Fig. 12.
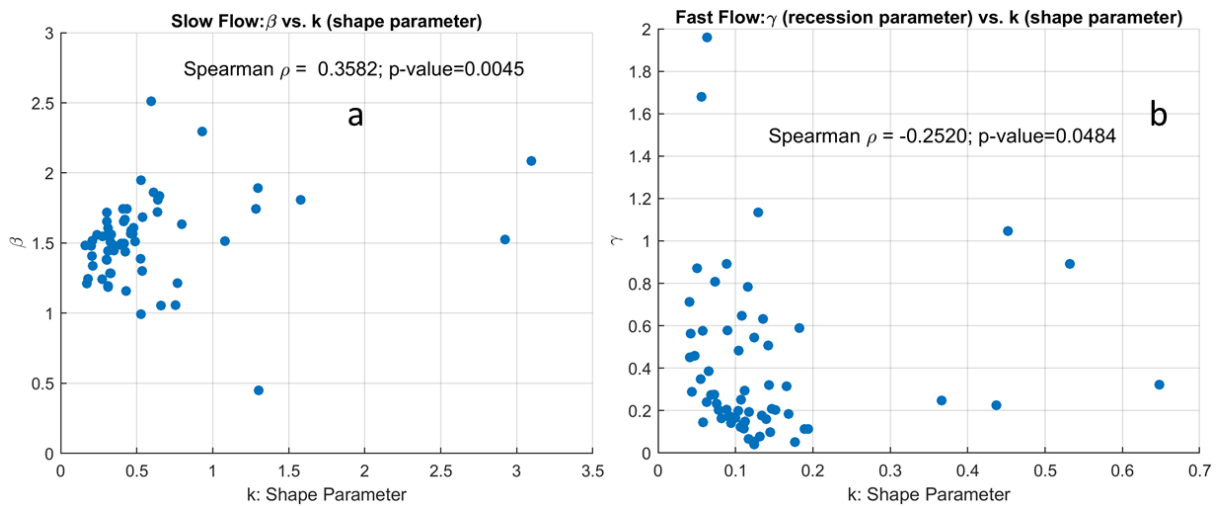
771

772 **Figure 11~~2~~.** Relationship between flow variability (related inversely to shape parameter, k of mixed gamma
773 distribution) and recession parameters.

774 ~~The variation of the parameters, k and α was also studied using spatial descriptors (latitude and longitude) as~~
775 ~~explanatory variables to understand the spatial variation of FDCs across south-north, west-east gradients. In~~
776 ~~addition, the behaviour of these parameters is also assessed using catchment area as another explanatory variable.~~
777 ~~The regional parameter sets comprising of k and α are next constructed for slow and fast flow processes by~~
778 ~~including these parameters for all the time series across different gauging stations across the Peninsular region.~~
779 ~~The Spearman correlation coefficients between these parameters and explanatory variables (i.e., catchment area~~
780 ~~and spatial descriptors – latitude and longitude) for slow and fast flow processes at seasonal scales are computed.~~
781 ~~The schematic representation of significant directions (positive/negative correlations) in Spearman coefficient is~~
782 ~~shown in Fig. 13.~~

783
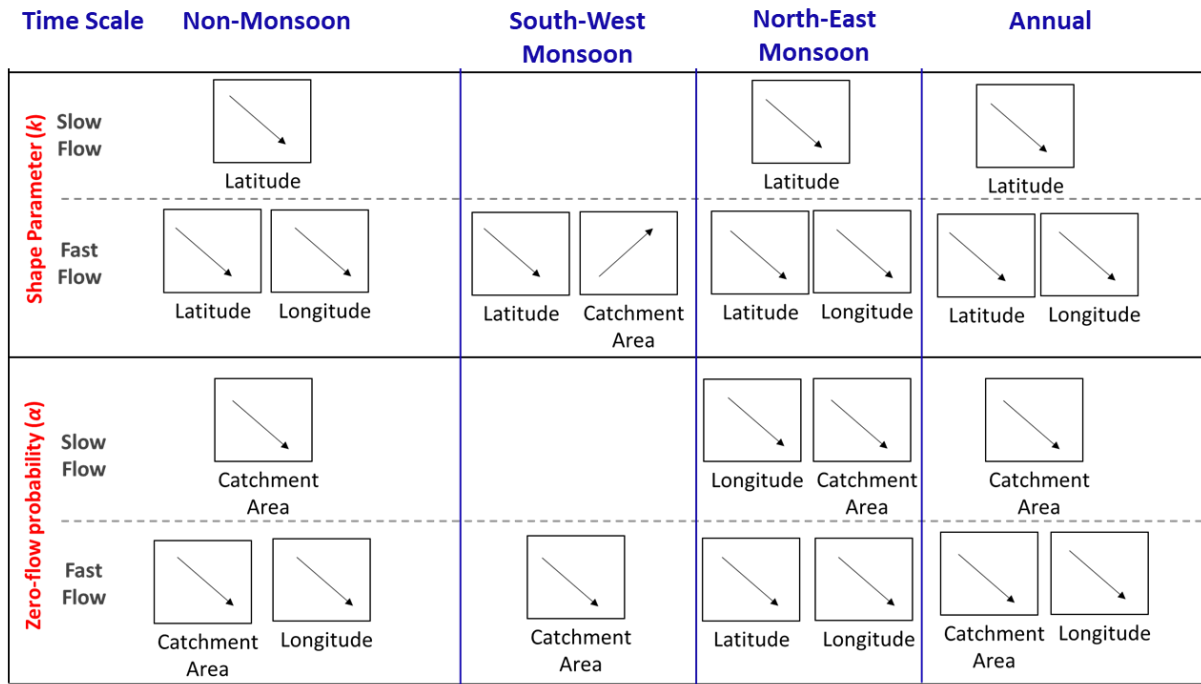
Figure 123. Schematic representation of spatial and temporal variation of parameters of mixed gamma distribution across Peninsular India. The direction of significant Spearman correlation coefficient between model parameters and descriptors (catchment area and spatial descriptors – latitude and longitude) for fast and slow flow across multiple time scale is presented.

The shape parameter of fast flow is found to be positively correlated with catchment area (Fig. 123, top panel), implying lower variability of fast flow in large catchments. This can be attributed to increased smoothening effect of incoming rainfall in larger catchments through various storages, thus reducing the variability of fast flow. Moreover, the shape parameters for fast flow are negatively correlated with spatial descriptors, indicating increased variability of fast flow along south-north and west-east gradients. This can be partly explained by the bimodal seasonal pattern of rainfall due to dominance of South-West and North-East monsoons, thus reducing the variability of fast flow in the southern part of the region. The rainfall pattern becomes more seasonal (primarily due to South-West monsoon) in the northern part of region which can contribute to increased variability of fast flow. The presence of numerous water retention structures for supporting irrigation in these regions (54 – 75% of Peninsular basins are crop land) can modify the variability of the flow, although we have not analysed this separately in this study.

The shape parameter of slow flow is found to be negatively correlated with latitude, implying that slow flow becomes highly variable in the northern part of the region. This can be explained by the nature of geologic formations in the Cauvery basin that promotes slow flow even during the Non-monsoon period. However, in the northern part of the region, the slow flow tends to become more seasonal and has very limited flow during non-rainy seasons. In addition to the geology, the bimodal seasonal rainfall patterns due to monsoons can play an important role in the variability of slow flow. Apart from the spatial descriptors, the slow flow variability is inversely proportional to catchment area, implying larger catchments have lower slow flow variability than smaller catchments. This can be explained by the proportional increase in area of contribution to slow flow with increase in catchment size, thus reducing the variability in slow flow for larger catchments.

809 The parameter α is found to be negatively correlated with catchment area (Fig. 1~~2~~3, bottom panel) for fast and
810 slow processes, implying zero-flow probabilities are lower for larger catchments. The higher residence time of
811 water in larger catchment due to various kinds of storages facilitates flow in river even in Non-monsoon season,
812 thus reducing the zero-flow probabilities. In addition, the parameter α of both slow and fast flow are negatively
813 correlated with longitude, implying lower zero-flow probabilities along west-east direction. This can be attributed
814 to natural declining elevation (Fig. S1.b) which promotes both fast and slow flow towards eastern direction.

815 **5.2 Understanding physical controls and spatial variation of seasonal flow duration curve using mid-section**
816 **slope**

817 Apart from mean, variance and no-flow frequency, the midsection slope of the FDC – estimated using
818 $\frac{\ln(Q_{33p})-\ln(Q_{66p})}{0.66-0.33}$, where Q_{33p} and Q_{66p} represent the streamflow values at 33rd and 66th percentiles respectively –
819 is connected to the average flow regime of the catchment, which is controlled by both surface and subsurface
820 processes (Yokoo & Sivapalan, 2011; Chouaib et al., 2018). The association of the slope of FDC with the
821 parameters pertaining to recession analysis is presented in Fig. 1~~3~~4.
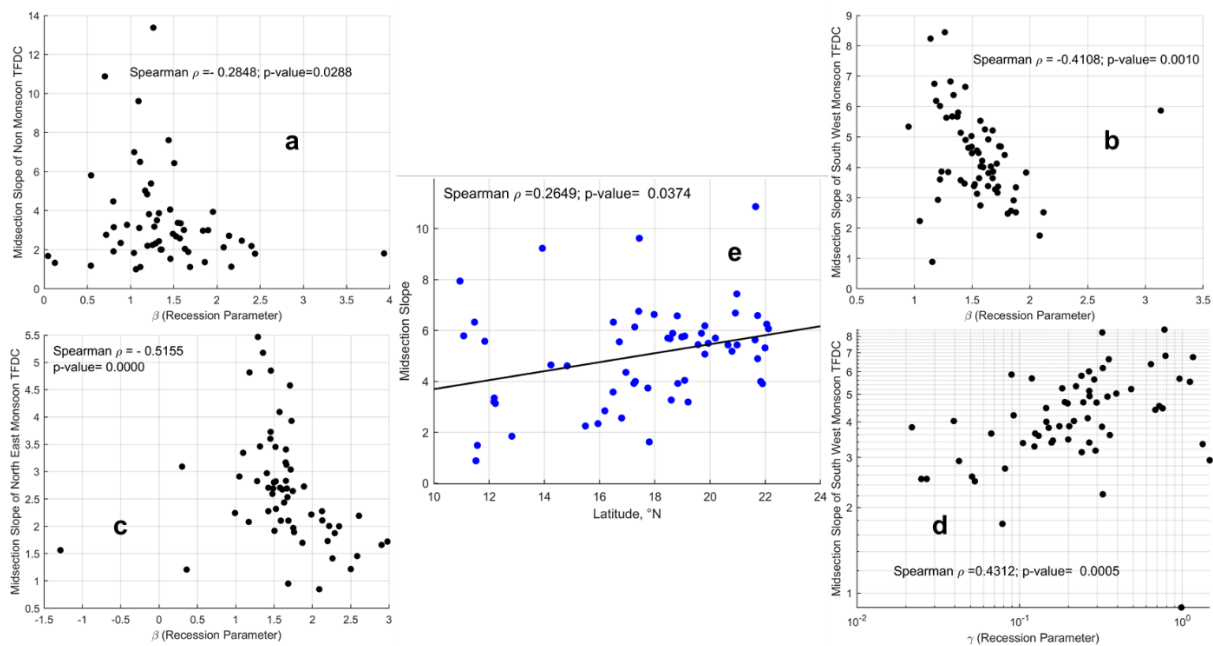
823 **Figure 1~~3~~4.** Association between streamflow variability and recession parameters.

824 During Non-monsoon and North East monsoon seasons (Fig. 1~~3~~4a and Fig. 1~~3~~4c) – when rainfall is comparatively
825 less than South West monsoon – a significant association between flow variability and β highlights the importance
826 of slow flow and recession characteristics controlled by aquifer geometry and water table elevation profile. In
827 addition to significant association with β during South West monsoon (Fig. 1~~3~~4b), the midsection slope of FDC
828 is positively correlated with γ – the parameter which is strongly related with the seasonality of catchment wetness,
829 evapotranspiration and spatial variation in rainfall – revealing the importance of land surface processes in
830 variability of streamflow variability.

A coherent pattern in variability of streamflow (via. Midsection slope of FDC) is observed across South – North gradient of the Peninsular region (Fig. 134e). This systematic pattern in streamflow variability reflects the influence of combined functioning of subsurface and land surface processes on regional hydrologic signatures of Peninsular India.

6. Conclusions

Being a signature of a catchment's hydrological behavior and a concise graphical summary of streamflow variability at a specific gauging station, FDC relates the frequency and magnitude of observed streamflows and helps explain flooding mechanisms and low flow conditions at the referred location. Furthermore, at the catchment scale, FDCs incorporate the forcing mechanisms of the water cycle and the physical and morphological properties of the river basin that influence the water partition between surface runoff and baseflow and, thus, control flow regimes (Costa & Fernandes, 2021). Motivated by this fact, in this study we outlined a framework and its suitability for understanding process controls of FDCs, which involved separating annual streamflow into seasonal flow components and constructing annual FDC using seasonal FDCs. The goal of this study was to demonstrate the efficacy of the framework to explore the process controls on streamflow variability across Peninsular India. The study followed a data-based approach using streamflow data taken from 62 stream gauges distributed within four major river basins in Peninsular India. The probability density functions are initially derived for daily streamflow time series for Non-monsoon, South West monsoon, and North East monsoon seasons. These PDFs are then multiplied by scaling factors that represent relative durations of the seasons considered. The probability density function of annual flow is then estimated as the weighted sum of three scaled density functions corresponding to three seasons. The performance of the time scale partitioning framework is then further assessed using the metric root mean square error.

Analysis and interpretation of the results of the study revealed that the main drivers of regional variability of streamflow across Peninsular India include (1) major mountain ranges – the Western and Eastern Ghats – which govern regional atmospheric circulation and precipitation variability; (2) the South West and North East monsoons that occur in different times of the year and come from different directions; and (3) east-west and north-south gradients of geology. The combined influence of seasonal rainfall patterns, catchment size and the ability of the subsurface formations to transmit slow flow controls the shape of flow duration curves of the flow components along south-north and west-east directions in Peninsular region.

To summarize, the major findings of the study are outlined below:

I.   Spatial variations of seasonal and annual flow duration curves across Peninsular India are initially investigated by approximating the annual flow duration curve via partitioned seasonal and monthly flow duration curves. FDCs of South-West monsoon flows are relatively dominant to other seasonal FDCs at stations in the northern portion of the peninsula. From June to September, flow contributions in northern Peninsular basins are significantly higher than in other months (Mahanadi and Godavari, Krishna to a lesser extent). However, the contribution from June to September is not as substantial in the southernmost Cauvery basin; there is also a major contribution from October to December. This is attributable to the fact that the South-West and North-East monsoons both impact the Cauvery basin. It is further noticed that the contribution of the North-East monsoon to annual flow is larger in southern basins than in

869   northern basins. The contribution of the Non monsoon to annual flow is also stronger in the southern

870   basin and is attributed to winter rains from the North East monsoon, which are more evident in the

871   southern part of the peninsula, creating carryover flows.

872 II.   The streamflow produced in the headwater regions of southern basins, which extends until 17° N latitude

873   and contributes at least 70% of the annual flow, is a result of high rainfall during the South-West monsoon

874   season in the mountainous region of the southern Peninsula (western part of Krishna basin and north-

875   western part of Cauvery basin). The northern part of the Peninsular region experiences notably higher

876   rainfall than the southern part, not considering the Western Ghats region. The low-pressure system, which

877   is a regular feature of the South-West monsoon that brings significant rainfall in the northern part of the

878   Peninsular region, attributes the increased rainfall (after 16° N latitude) and is responsible for the higher

879   contribution of South-West monsoon flows to annual flow in the northern basins. The spatial variation in

880   the contribution of South-West monsoon flows to annual flow in the south-north direction is thus

881   explained by the spatial variability of the South-West monsoon in the same direction over the Peninsular

882   region. The contribution of North East monsoon flows to annual flow, on the other hand, increases in a

883   southerly direction, which can be explained by the fact that the southern part of the Peninsular region

884   receives more rainfall during the North-East monsoon than the rest of the Peninsular region.

885 III.   Spatial variations of fast/slow and total flow duration curves across Peninsular India are then explored

886   by approximating the total flow duration curve by partitioned flow duration curves. Relative

887   contributions of fast and slow flows to total flow in each of the four river basins show a significant

888   dominance of fast flow in the northern basins, close to 80% in Mahanadi, Godavari, and Krishna river

889   basins.

890 IV.   The Western Ghats, which run along the western boundary of the Krishna and Cauvery basins, bring a

891   lot of rain to the southern part of the region. As a result, the western margins of the sub-basins along the

892   Krishna basin contribute 80 percent of the fast flow to total flow (between 13° N and 18°N latitudes).

893   However, the south-north gradient in fast flow contributions to total flow is governed by increasing

894   spatial mean characteristics of annual rainfall after 16° N latitude, which dictates an increased

895   contribution of fast flow to total flow.

896 V.   The greater contribution of slow flow to total flow in the southern Peninsular region, particularly Cauvery

897   and Krishna, is characterized by bimodal rainfall seasonality and the presence of a higher fraction of

898   moderate to good groundwater potential zones and is responsible for the spatial variation of

899   increased relative contributions of slow flow to total flow in the southerly direction over the Peninsular

900   region.

901 VI.   A coherent pattern in streamflow variability across the South North gradient of the Peninsular region is

902   observed via the midsection slope of FDC. These similar spatial variation in streamflow variability

903   demonstrate the impact of combined subsurface and land surface processes on Peninsular India's regional

904   hydrologic signatures.

905 Previous data-based explorations of process controls on the FDC have typically followed a Darwinian (Harman

906 and Troch, 2014) comparative hydrology approach. They have looked at between catchment and regional

907 variations of the FDC (or of parameters of statistical distributions fitted to empirical FDCs), their attribution to

908 climatic and landscape properties, and their interpretation in terms of their underlying process controls (fast flow

909 and slow flow etc). In the Darwinian approach, each catchment is deemed a particular but statistically independent
910 realization of the coevolution of climate and landscape properties, with the hydrologic response being both a cause
911 and effect in this coevolution (Wagener et al., 2013). The novelty of the data-based exploration of process controls
912 on the FDC adopted in this study is that here we have followed a Wegenerian (cf. Alfred Wegener, Sivapalan,
913 2018) comparative hydrology approach, in which the focus was on exploration of the controls of common regional
914 landscape features (in space) and seasonal climatic variations (in time) features on regional variations of the FDC.
915 We interpret the imprints of the regional variations streamflow variability of the FDCs outlined as findings across
916 Peninsular India as the consequence of several episodes of tectonic, geological, and volcanic activities in the
917 Indian subcontinent ever since the breakup of Gondwana and its collision with Asia during the Jurassic age,
918 resulting in the uplift of mountain ranges, including the Himalayas, and their role in the establishment of India's
919 monsoon climate.

920 The comprehensive analysis of spatial variations in seasonal and annual flow duration curves across Peninsular
921 India has provided valuable insights into the controls of streamflow variability at different scales. The partitioning
922 framework employed in this study effectively approximated annual flow duration curves, confirming its efficacy
923 in capturing the intricate dynamics of seasonal and monthly flows. Noteworthy spatial patterns emerged, with
924 gauging stations in the northern part of the peninsula exhibiting higher dominance of South-West monsoon flows
925 in contrast to the more balanced contributions observed in the southern regions, where North-East monsoon flows
926 also played a significant role.

927 The regional-scale analysis unveiled the influence of spatial patterns of monsoon rainfall, showing increased
928 contributions of South-West monsoon flows in the northerly direction and elevated contributions of North-East
929 monsoon flows in the southerly direction. The study also delved into the partitioning of streamflow into fast and
930 slow components, revealing a dominance of fast flow in northern basins and an increasing contribution of slow
931 flow in the southerly direction. Factors such as rainfall intensity, geologic formations, and groundwater gradients
932 were identified as critical controls shaping these flow characteristics. The investigation of combined influences
933 of climatic time scales and process time scales further enriched our understanding of streamflow variability.
934 Seasonal fluctuations in fast and slow flow contributions highlighted the dynamic nature of streamflow response
935 to monsoon onset and withdrawal. The study emphasized the importance of considering both climatic and
936 landscape factors across different scales to comprehensively grasp the controls of streamflow variability in the
937 Peninsular region.

938 By undertaking an extensive analysis of flow duration curves for both fast and slow flow components across
939 different seasons, the study aims to understand the variations and controls governing these hydrological patterns.
940 The initial step of scaling the fast and slow flow time series by their respective long-term mean values serves as
941 a crucial tool in isolating secondary controls on FDC shapes, effectively removing the influence of mean climate
942 and geology. The subsequent use of the Mixed Gamma Distribution to fit the scaled time series allows for an
943 advanced examination of the parameters influencing FDC shapes, with a focus on the key factors of shape
944 parameter (k) and probability of zero flows (α). The seasonal variations of MGD parameters at a regional scale
945 reveal the impact of monsoons on streamflow characteristics. Notably, the consistently higher shape parameters
946 for slow flow highlight the lower variance attributed to longer residence times in subsurface formations,
947 emphasizing the influence of geological features.

Further exploration into the relationships between MGD parameters and landscape properties through recession analysis enhances our understanding of hydrological controls. The positive correlation between the shape parameter of slow flow and recession parameter β, influenced by aquifer geometry, contrasts with the negative correlation between the shape parameter of fast flow and the parameter γ, associated with seasonality of catchment wetness and evapotranspiration. Spatial variation analysis using descriptors like latitude, longitude, and catchment area unveils significant correlations, offering insights into the influence of geographical factors on FDC shapes. The correlation of fast flow shape parameters with catchment area suggests reduced variability in larger catchments, while the negative correlation of slow flow shape parameters with latitude indicates increased variability in the northern part of the region. The examination of zero-flow probabilities controlled by the parameter α reveals noteworthy trends. Larger catchments exhibit lower zero-flow probabilities, and the negative correlation of α with longitude highlights the spatial influence along the west-east direction. Finally, the study explores the midsection slope of the FDC, connecting it to average flow regimes controlled by both surface and subsurface processes. Associations with recession analysis parameters underline the integrated influence of aquifer geometry and land surface processes on streamflow variability across Peninsular India.

In summary, the methodology employed in this study offers a systematic and insightful approach to unravelling the complexities of streamflow variability across Peninsular India. This study not only enhances our understanding of the relative contributions and shapes of FDCs but also sheds light on the intricate interplay of geological, spatial, and hydrological factors influencing streamflow variability in this region.

We acknowledge, however, that in recent times streamflow variability in Peninsular India has been significantly impacted by anthropogenic activities, including significant land use and land cover changes, and other human interferences such as the building of dams and the extraction of water from both rivers and from groundwater aquifers for human use. The present study has not explored the effects of human impacts: their impacts on both temporal (inter-decadal) and spatial (regional) variations of the FDCs is left for future work. Further work is also needed to understand in more detail the causes and the relative contributions of regional patterns precipitation and geological formations on streamflow partitioning.

On the methodological front, there is opportunity to refine the analysis used here to incorporate the statistical cross-correlation between fast and slow flows in the reconstruction of the FDC for total streamflow, by adopting generalized approaches (e.g., copulas). In the exploration of the relative contributions of the monsoons, there is scope to extend the analysis framework to partition the streamflow variability guided by the actual breakdown into the seasons each year in a more flexible way, as opposed to the static way. This is likely to make the results of the analysis more robust and less uncertain. Finally, in the process domain, the filter-based separation of total streamflow into fast and slow flow can be variably impacted by catchment size, introducing some uncertainty into the partitioning of the FDC of total streamflow into its fast flow and slow flow components. Future work in this area should explore ways to overcome these methodological shortcomings.

Appendix

A.1 Baseflow decomposition (Recursive Digital Filter)

985 The partitioning of total flow (Q) into slow flow (Q_s) is performed using recursive digital filter technique as

986 described in Arnold & Allen (1999) and Arnold et al. (1995). Based on the study by Nathan and McMahon (1990),

987 they found that a coefficient range between 0.9 and 0.95 yielded most acceptable baseflow separation. Therefore,

988 we have taken the value 0.95 as a coefficient value for this analysis (more discussion is provided at the end of

989 A.1). This filter is applied to daily streamflow timeseries data for all the gauging stations across the Peninsular

990 region.

991 The equation of the filter is

992 $$q_t = \varepsilon q_{t-1} + \frac{(1+\varepsilon)}{2}(Q_t - Q_{t-1}) \qquad \text{(A.1)}$$

993 where q_t is the filtered surface runoff (quick response) at the t time step, Q is the original streamflow (total flow),

994 and ε is the filter parameter (which is assumed to be 0.95). Slow flow, Q_s, is calculated with the equation:

995 $$Q_s = Q - q_t \qquad \text{(A.2)}$$

996 After obtaining the slow flow component, the fast flow (Q_f) is obtained by subtracting Q_s from Q.

997 $$Q_f = Q - Q_s \qquad \text{(A.3)}$$

998 In order to demystify the role of different values of the filter parameter in the digital recursive filter, the model

999 was run for three different seasons for all the catchments in Peninsular region. The results are presented in Figure

1000 A1.
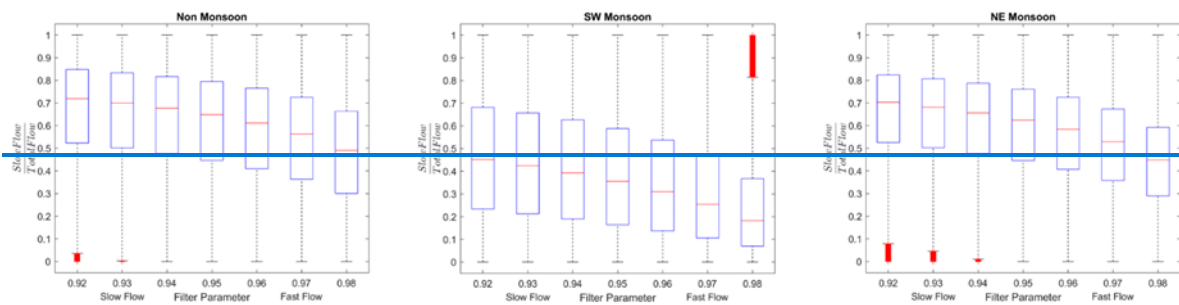
1001

1002 **Figure A1.** Contribution of slow flow to total flow for different seasons. The box plots in each season represent
1003 the partitioning of total flow into slow flow for different filter parameters, viz. [0.92,0.93,0.94,0.95,0.96,0.97
1004 ,0.98].
1005

1006 It is observed that the median variations in the slow flow fraction during non monsoon period (0.5-0.7), south

1007 west monsoon period (0.18-0.45) and north east monsoon period (0.44-0.7) which lies within 30% variation.

1008 However, even with these variations, the overall pattern, i.e., high slow flow contribution during non monsoon

1009 and north east monsoon seasons and low slow flow contribution during south west monsoon remains intact,

1010 revealing seasonal changes in the dynamics of slow flow contribution to total flow. In this paper, we assumed the

1011 parameter 0.95 reflecting the average variability in slow flow contributions to total flow.

1012 A.2 Recession Analysis

1013 In recession analysis, it is often assumed that rate of change of streamflow $\frac{dQ}{dt}$ and streamflow (Q) follows a

1014 power law in the form:

1015 $$-\frac{dQ}{dt} = \gamma Q^\beta \qquad \text{(A.4)}$$

1016 The parameter γ is function of static watershed properties (i.e., hydrological conductivity, drainable porosity,

1017 aquifer depth, aquifer breadth, impermeable layer slope and length of stream) (Tashie et al., 2020a). The parameter

β represents the geometry of the contributing aquifer and water table elevation profile that defines the early and late periods of recession (Tashie et al., 2020b). $\frac{dQ}{dt}$ is estimated using exponential time stepping scheme (Roques et al., 2017). Strictly decreasing recession segments ($\frac{dQ}{dt} < 0$) with recession segments more than 5 days are considered for the estimation of the parameters (γ and β) (Jachens et al., 2020). A weighted least square regression is used to fit a line in log-log space to recession segments (Roques et al., 2017). The median of the parameters is used to describe catchment-average recession behaviour (Gnann et al., 2021).

A.3 Absolute contributions of fast and slow flow to total flow

The absolute contributions of fast and slow flow to total flow are determined using the coefficient of determination (R^2) of simple linear regression models, that measures the reduction in variability of total flow due to fast and slow flow components. The details are given below:

Model 1: $Q = \varphi_1 \cdot Q_f + c_1$ (A.5)

Model 2: $Q = \varphi_2 \cdot Q_s + c_2$ (A.6)

The coefficient of determination measures the effect of slow(fast) flow in reducing the variation in total flow based on Model1(Model2). Higher the value of this coefficient, higher the contribution of slow/fast flow in reducing the variation in total flow.

The coefficient of determinations for two models can be estimated as:

$$R^2_{(1)} = \frac{SSR^{(1)}}{SSTO}$$ (A.7)

$$R^2_{(2)} = \frac{SSR^{(2)}}{SSTO}$$ (A.8)

where, $SSR^{(1)}$ and $SSR^{(2)}$ represent the regression sum of squares for Model 1 and Model 2 respectively, and SSTO represents the total sum of squared deviations from mean, i.e., $SSTO = \sum(Q_t - \bar{Q})^2$. The sum of squares due to the models are expressed as:

$SSR^{(1)} = \sum(\widehat{Q_{(1)}} - \bar{Q})^2$ and $SSR^{(2)} = \sum(\widehat{Q_{(2)}} - \bar{Q})^2$ where $\widehat{Q_{(1)}}$ and $\widehat{Q_{(2)}}$ are the fitted values of total flow using Model 1 and Model 2 respectively.

The values of coefficient of determination (R^2) for three seasons are shown in Fig. A2.

Absolute contributions of fast and slow flow to total flow

Peninsular India

45

distribution is a two-parameter, continuous distribution with a shape parameter, k, and a scale parameter, θ. In addition, the probability of zero flows, α, is defined as the ratio of the number of zero flow days to the total number of days within the data record. The mixed gamma distribution (Cheng et al., 2012) employed to model FDC is as follows:

$$f(q, k, \theta, \alpha) = \begin{cases} \alpha, & q = 0 \\ (1 - \alpha) \cdot g(q, k, \theta), & q > 0 \end{cases} \tag{A.9}$$

where $g(q, k, \theta)$ is the probability density function of the gamma distribution. The probability density function of the gamma distribution is assumed to take the form of (Cheng et al., 2012):

$$g(q, k, \theta) = \frac{1}{|\theta| \, \Gamma(k)} \left(\frac{q}{\theta}\right)^{k-1} \exp\left(-\frac{q}{\theta}\right) \tag{A.10}$$

where k and θ are the shape and scale parameters, respectively. The parameters k and θ can be estimated by the method of moments. The mean, μ, and variance, ν, of the gamma distribution are evaluated from the $q > 0$ time series. The parameters are related to μ and ν as follows:

$$\mu = k \cdot \theta \tag{A.11}$$

$$\nu = k \cdot \theta^2 \tag{A.12}$$

The following formulation is used to obtain the flow given a probability of exceedance, p (Cheng et al., 2012):

$$q(p, k, \theta, \alpha) = \begin{cases} G^{-1}\left(1 - \frac{p}{1 - \alpha}, k, \theta\right), & 0 \le p \le 1 - \alpha \\ 0, & 1 - \alpha < p \le 1 \end{cases} \tag{A.13}$$

where G^{-1} is the inverse of the CDF of the mixed gamma distribution.

In this case, given that we have already looked at the climatic and landscape controls on the mean annual flows, we instead work with the normalized daily streamflow time series (i.e., daily streamflow divided by long-term mean daily streamflow), which is then used to estimate the parameters of the mixed gamma distribution. The parameters estimated from the normalized streamflow series can thus be used to infer secondary controls on the shape of flow duration curves.

A.5 Investigating the slow flow fraction of total flow in Peninsular India

The variability in slow flow fraction (SFF) is investigated using multiple linear regression by considering the recession parameters, β and γ in the equation $-\frac{dQ}{dt} = \gamma Q^\beta$ and the location of the gauge (δ, latitude). The results are provided below:

Regression Model:

$$SFF = \alpha_0 + \alpha_1 \gamma + \alpha_2 \beta + \alpha_3 \delta \tag{A.14}$$

Table A.1 Statistical Assessment of regression coefficients

Coefficients	Estimate	SE	tStat	pValue
α_0, (Intercept)	0.35361	0.055275	6.3973	2.99E-08
α_1	-0.024117	0.021119	-1.142	0.25816
α_2	0.12791	0.025704	4.9764	6.12E-06
α_3	-0.015556	0.0023978	-6.4875	2.12E-08

The above regression model was able to explain to about 52% of the variability in slow flow fraction of total flow (p-value = 1.98×10^{-9}), and in general, the model is found to be useful to explain SFF in terms of recession parameter and latitude. A fraction of the unexplainable part in SFF can be attributed to the heterogeneity in subsurface geologic formations and dam-induced variations in the catchment storages. However, at a regional scale, the south-north gradient (represented by the parameter δ) can explain the variability in slow flow fraction to total flow. This regional setting is an important outcome to understand the streamflow variability in Peninsular region of India.

References

Arai, R., Toyoda, Y., & Kazama, S. (2021). Runoff recession features in an analytical probabilistic streamflow model. Journal of Hydrology, 597, 125745.

Arnold, J. G. and Allen, P. M.: Automated methods for estimating baseflow and ground water recharge from streamflow records, J. Am. Water Resour. Assoc., 35, 411–424, https://doi.org/10.1111/j.1752-1688.1999.tb03599.x, 1999.

Arnold, J. G., Allen, P. M., Muttiah, R., and Bernhardt, G.: Automated Base Flow Separation and Recession Analysis Techniques, Ground Water, 33, 1010–1018, https://doi.org/10.1111/j.1745-6584.1995.tb00046.x, 1995.

Arulbalaji, P., Sreelash, K., Maya, K., and Padmalal, D.: Hydrological assessment of groundwater potential zones of Cauvery River Basin, India: a geospatial approach, Environ. Earth Sci., 78, 1–21, https://doi.org/10.1007/s12665-019-8673-6, 2019.

Basso, S. and Botter, G.: Streamflow variability and optimal capacity of run-of-river hydropower plants, Water Resour. Res., 48, 1–13, https://doi.org/10.1029/2012WR012017, 2012.

Basso, S., Schirmer, M., & Botter, G. (2015). On the emergence of heavy-tailed streamflow distributions. Advances in Water Resources, 82, 98-105.

Bhardwaj, K., Shah, D., Aadhar, S., and Mishra, V.: Propagation of Meteorological to Hydrological Droughts in India, J. Geophys. Res. Atmos., 125, https://doi.org/10.1029/2020JD033455, 2020.

Biswal, B. and Nagesh Kumar, D.: Study of dynamic behaviour of recession curves, Hydrol. Process., 28, 784–792, https://doi.org/10.1002/hyp.9604, 2014.

Blum, A. G., Archfield, S. A., Vogel, R. M., and Survey, G.: On the probability distribution of daily streamflow in the United States, Hydrol. Earth Syst. Sci., 21, 3093–3103, https://doi.org/https://doi.org/10.5194/hess-21-3093-2017, 2017.

Botter, G., Zanardo, S., Porporato, A., Rodriguez-Iturbe, I., and Rinaldo, A.: Ecohydrological model of flow duration curves and annual minima, Water Resour. Res., 44, 1–12, https://doi.org/10.1029/2008WR006814, 2008.

Botter, G., Basso, S., Rodriguez-Iturbe, I., & Rinaldo, A. (2013). Resilience of river flow regimes. Proceedings of the National Academy of Sciences, 110(32), 12925-12930.

Carlier, C., Wirth, S. B., Cochand, F., Hunkeler, D., & Brunner, P. (2018). Geology controls streamflow dynamics. Journal of Hydrology, 566, 756-769.

Chanapathi, T. and Thatikonda, S.: Investigating the impact of climate and land-use land cover changes on hydrological predictions over the Krishna river basin under present and future scenarios, Sci. Total Environ., 721, 137736, https://doi.org/10.1016/j.scitotenv.2020.137736, 2020.

Chandra, P. C.: Groundwater of Hard Rock Aquifers of India, 61–84, https://doi.org/10.1007/978-981-10-3889-1_5, 2018.

Chatterjee, S., Scotese, C. R., and Bajpai, S.: The Restless Indian plate and its epic voyage from Gondwana to Asia: Its tectonic, paleoclimatic, and paleobiogeographic evolution, Spec. Pap. Geol. Soc. Am., 529, 1–147, https://doi.org/10.1130/2017.2529, 2017.

Cheng, L., Yaeger, M., Viglione, A., Coopersmith, E., Ye, S., and Sivapalan, M.: Exploring the physical controls of regional patterns of flow duration curves – Part 1: Insights from statistical analyses, Hydrol. Earth Syst. Sci., 16, 4435–4446, https://doi.org/10.5194/hess-16-4435-2012, 2012.

Chouaib, W., Caldwell, P. V., and Alila, Y.: Regional variation of flow duration curves in the eastern United States: Process-based analyses of the interaction between climate and landscape properties, J. Hydrol., 559, 327–346, https://doi.org/10.1016/j.jhydrol.2018.01.037, 2018.

Collins, L. S., Loveless, S. E., Muddu, S., Buvaneshwari, S., Palamakumbura, R. N., Krabbendam, M., Lapworth, D. J., Jackson, C. R., Gooddy, D. C., Nara, S. N. V., Chattopadhyay, S., and MacDonald, A. M.: Groundwater connectivity of a sheared gneiss aquifer in the Cauvery River basin, India, Hydrogeol. J., 28, 1371–1388, https://doi.org/10.1007/s10040-020-02140-y, 2020.

Costa, V. and Fernandes, W.: Regional Modeling of Long-Term and Annual Flow Duration Curves: Reliability for Information Transfer with Evolutionary Polynomial Regression, J. Hydrol. Eng., 26, 1–12, https://doi.org/10.1061/(asce)he.1943-5584.0002051, 2021.

Das, S.: Frontiers of Hard Rock Hydrogeology in India, in: Ground Water Development - Issues and Sustainable Solutions, Springer Singapore, Singapore, 35–68, https://doi.org/10.1007/978-981-13-1771-2_3, 2019.

Deshpande, N. R., Kothawale, D. R., and Kulkarni, A.: Changes in climate extremes over major river basins of India, Int. J. Climatol., 36, 4548–4559, https://doi.org/10.1002/joc.4651, 2016.

Dralle, D., Karst, N., and Thompson, S. E.: a, b careful: The challenge of scale invariance for comparative analyses in power law models of the streamflow recession, Geophys. Res. Lett., 42, 9285–9293, https://doi.org/10.1002/2015GL066007, 2015.

Durighetto, N., Mariotto, V., Zanetti, F., McGuire, K. J., Mendicino, G., Senatore, A., & Botter, G. (2022). Probabilistic description of streamflow and active length regimes in rivers. Water Resources Research, 58, e2021WR031344. https:// doi.org/10.1029/2021WR031344

Gadgil, S.: The Indian Monsoon and Its Variability, Annu. Rev. Earth Planet. Sci., 31, 429–467, https://doi.org/10.1146/annurev.earth.31.100901.141251, 2003.

Fenicia, F., Kavetski, D., Savenije, H. H., Clark, M. P., Schoups, G., Pfister, L., & Freer, J. (2014). Catchment properties, function, and conceptual model representation: is there a correspondence? Hydrological Processes, 28(4), 2451-2467.

Ghotbi, S., Wang, D., Singh, A., Blöschl, G., and Sivapalan, M.: A New Framework for Exploring Process Controls of Flow Duration Curves, Water Resour. Res., 56, https://doi.org/10.1029/2019WR026083, 2020a.

Ghotbi, S., Wang, D., Singh, A., Mayo, T., and Sivapalan, M.: Climate and Landscape Controls of Regional Patterns of Flow Duration Curves Across the Continental United States: Statistical Approach, Water Resour. Res., 56, https://doi.org/10.1029/2020WR028041, 2020b.

Gnann, S. J., McMillan, H. K., Woods, R. A., and Howden, N. J. K.: Including Regional Knowledge Improves Baseflow Signature Predictions in Large Sample Hydrology, Water Resour. Res., 57, https://doi.org/10.1029/2020WR028354, 2021.

Gupta, H., Reddy, K. K., Gandla, V., Paridula, L., Chiluka, M., and Vashisth, B.: Freshwater discharge from the large and coastal peninsular rivers of India: A reassessment for sustainable water management, Environ. Sci. Pollut. Res., 29, 14400–14417, https://doi.org/10.1007/s11356-021-16811-0, 2022.

Harini, P., Sahadevan, D. K., Das, I. C., Manikyamba, C., Durgaprasad, M., and Nandan, M. J.: Regional Groundwater Assessment of Krishna River Basin Using Integrated GIS Approach, J. Indian Soc. Remote Sens., 46, 1365–1377, https://doi.org/10.1007/s12524-018-0780-4, 2018.

Harman, C. and Troch, P. A.: What makes Darwinian hydrology "Darwinian"? Asking a different kind of question about landscapes, Hydrol. Earth Syst. Sci., 18, 417–433, https://doi.org/10.5194/hess-18-417-2014, 2014.

Kale, V. S., Hire, P., and Baker, V. R.: Flood Hydrology and Geomorphology of Monsoon-dominated Rivers: The Indian Peninsula, Water Int., 22, 259–265, https://doi.org/10.1080/02508069708686717, 1997.

Kale, V. S., Vaidyanadhan, R.: Landscapes and Landforms of India, edited by: Kale, V. S., Springer Netherlands, Dordrecht, 105–113 pp., https://doi.org/10.1007/978-94-017-8029-2_6, 2014.

Koneti, S., Sunkara, S. L., and Roy, P. S.: Hydrological modeling with respect to impact of land-use and land-cover change on the runoff dynamics in Godavari river basin using the HEC-HMS model, ISPRS Int. J. Geo-Information, 7, https://doi.org/10.3390/ijgi7060206, 2018.

Krishnamurthy, V. and Ajayamohan, R. S.: Composite Structure of Monsoon Low Pressure Systems and Its Relation to Indian Rainfall, J. Clim., 23, 4285–4305, https://doi.org/10.1175/2010JCLI2953.1, 2010.

Kumar Raju, B. C. and Nandagiri, L.: Analysis of historical trends in hydrometeorological variables in the upper Cauvery Basin, Karnataka, India, Curr. Sci., 112, 577–587, https://doi.org/10.18520/cs/v112/i03/577-587, 2017.

Krasovskaia, I., Gottschalk, L., Leblois, E., & Pacheco, A. (2006). Regionalization of flow duration curves. Climate variability and change: hydrological impacts, 105-110.

Leong, C., & Yokoo, Y. (2019). An interpretation of the relationship between dominant rainfall-runoff processes and the shape of flow duration curve by using data-based modeling approach. Hydrological Research Letters, 13(4), 62-68.

Leong, C., & Yokoo, Y. (2022). A multiple hydrograph separation technique for identifying hydrological model structures and an interpretation of dominant process controls on flow duration curves. Hydrological Processes, 36(4), e14569. https://doi.org/10.1002/hyp.14569

Magilligan, F. J. and Nislow, K. H.: Changes in hydrologic regime by dams, Geomorphology, 71, 61–78, https://doi.org/10.1016/j.geomorph.2004.08.017, 2005.

Magilligan, F. J., Nislow, K. H., and Graber, B. E.: Scale-independent assessment of discharge reduction and riparian disconnectivity following flow regulation by dams, Geology, 31, 569, https://doi.org/10.1130/0091-7613(2003)031<0569:SAODRA>2.0.CO;2, 2003.

Milliman JD, F. K.: River discharge to the coastal ocean: a global synthesis, river discharge to the coastal ocean: a global synthesis, Cambridge University Press, 2011.

1216 Müller, M. F., & Thompson, S. E. (2016). Comparing statistical and process-based flow duration curve models in
1217 ungauged basins and changing rain regimes. Hydrology and Earth System Sciences, 20(2), 669-683.

1218 Narasimhan, T. N.: Ground Water in Hard-Rock Areas of Peninsular India: Challenges of Utilization, Ground
1219 Water, 44, 130–133, https://doi.org/10.1111/j.1745-6584.2005.00167.x, 2006.

1220 Nathan, R. J. and McMahon, T. A.: Evaluation of automated techniques for base flow and recession analyses,
1221 Water Resour. Res., 26, 1465–1473, https://doi.org/10.1029/WR026i007p01465, 1990.

1222 Pai, D. S., Sridhar, L., Rajeevan, M., Sreejith, O. P., Satbhai, N. S., and Mukhopadhyay, B.: Development of a
1223 new high spatial resolution (0.25° × 0.25°) long period (1901-2010) daily gridded rainfall data set over India and
1224 its comparison with existing data sets over the region, Mausam, 1, 1–18, 2014.

1225 Patil, S., Kulkarni, H., Bhave, N., Development, W. R., Forum, P., Dialogue, P., and Conflicts, W.: Groundwater
1226 in the Mahanadi River Basin, https://doi.org/10.13140/RG.2.2.11561.95846, 2017.

1227 Prakash, S., Mitra, A. K., and Pai, D. S.: Comparing two high-resolution gauge-adjusted multisatellite rainfall
1228 products over India for the southwest monsoon period, Meteorol. Appl., 22, 679–688,
1229 https://doi.org/10.1002/met.1502, 2015.

1230 Rajeevan, M., Unnikrishnan, C. K., Bhate, J., Niranjan Kumar, K., and Sreekala, P. P.: Northeast monsoon over
1231 India: variability and prediction, Meteorol. Appl., 19, 226–236, https://doi.org/10.1002/met.1322, 2012.

1232 Ramachandra, T. V: Global Biodiversity Hotspot - Western Ghats : Water Tower of Peninsular India and Precious
1233 Heritage for Posterity, 2018.

1234 Rao, P. G., Chanapathi, T., Thatikonda, S., Koneti, S., Sunkara, S. L., Roy, P. S., Kumar Raju, B. C., and
1235 Nandagiri, L.: Investigating the impact of climate and land-use land cover changes on hydrological predictions
1236 over the Krishna river basin under present and future scenarios, Curr. Sci., 7, 577–587,
1237 https://doi.org/10.18520/cs/v112/i03/577-587, 2017.

1238 Rehana, S. and Mujumdar, P. P.: River water quality response under hypothetical climate change scenarios in
1239 Tunga-Bhadra river, India, Hydrol. Process., 25, 3373–3386, https://doi.org/10.1002/hyp.8057, 2011.

1240 Rehana, S. and Mujumdar, P. P.: Climate change induced risk in water quality control problems, J. Hydrol., 444–
1241 445, 63–77, https://doi.org/10.1016/j.jhydrol.2012.03.042, 2012.

1242 Richards, F. D., Hoggard, M. J., and White, N. J.: Cenozoic epeirogeny of the Indian peninsula, Geochemistry,
1243 Geophys. Geosystems, 17, 4920–4954, https://doi.org/10.1002/2016GC006545, 2016.

1244 Saha, K. R., Mooley, D. A., and Saha, S.: The Indian monsoon and its economic impact, GeoJournal, 3,
1245 https://doi.org/10.1007/BF00257706, 1979.

1246 Santos, A. C., Portela, M. M., Rinaldo, A., & Schaefli, B. (2018). Analytical flow duration curves for summer
1247 streamflow in Switzerland. Hydrology and earth system sciences, 22(4), 2377-2389.

1248 Searcy, J. K.: Flowduration curves, Man. Hydrol. U.S. Geol. Surv., 1959.

1249 Sinha, J., Sharma, A., Khan, M., and Goyal, M. K.: Assessment of the impacts of climatic variability and
1250 anthropogenic stress on hydrologic resilience to warming shifts in Peninsular India, Sci. Rep., 8, 13833,
1251 https://doi.org/10.1038/s41598-018-32091-0, 2018.

1252 Sivapalan, M.: From engineering hydrology to Earth system science: milestones in the transformation of
1253 hydrologic science, Hydrol. Earth Syst. Sci., 22, 1665–1693, https://doi.org/10.5194/hess-22-1665-2018, 2018.

1254 Smakhtin, V. U.: Smakhtin 2010- Low flow hydrology.pdf, J. Hydrol. Hydrol., 240, 147–186,
1255 https://doi.org/10.1016/S0022-1694(00)00340-1, 2001.

1256 Sreelash, K., Mathew, M. M., Nisha, N., Arulbalaji, P., Bindu, A. G., and Sharma, R. K.: Changes in the
1257 hydrological characteristics of Cauvery river draining the eastern side of southern Western Ghats, India, Int. J.
1258 River Basin Manag., 18, 153–166, https://doi.org/10.1080/15715124.2020.1719119, 2020.

1259 Stewart, M. K. (2015). Promising new baseflow separation and recession analysis methods
1260 applied to streamflow at Glendhu Catchment, New Zealand. Hydrology and Earth System
1261 Sciences, 19(6), 2587-2603.

1262 Tashie, A., Pavelsky, T., and Band, L. E.: An Empirical Reevaluation of Streamflow Recession Analysis at the
1263 Continental Scale, Water Resour. Res., 56, https://doi.org/10.1029/2019WR025448, 2020a.

1264 Tashie, A., Pavelsky, T., and Emanuel, R. E.: Spatial and Temporal Patterns in Baseflow Recession in the
1265 Continental United States, Water Resour. Res., 56, https://doi.org/10.1029/2019WR026425, 2020b.

1266 Tongal, H., Demirel, M. C., and Moradkhani, H.: Analysis of dam-induced cyclic patterns on river flow dynamics,
1267 Hydrol. Sci. J., 62, 626–641, https://doi.org/10.1080/02626667.2016.1252841, 2017.

1268 Vogel, R. M. and Fennessey, N. M.: Flow-Duration Curves. I: New Interpretation and Confidence Intervals, J.
1269 Water Resour. Plan. Manag., 120, 485–504, https://doi.org/10.1061/(ASCE)0733-9496(1994)120:4(485), 1994.

1270 Vogel, R. M. and Fennessey, N. M.: Flow Duration Curves Ii: a Review of Applications in Water Resources
1271 Planning, JAWRA J. Am. Water Resour. Assoc., 31, 1029–1039, https://doi.org/10.1111/j.1752-
1272 1688.1995.tb03419.x, 1995.

1273 Wagener, T., Blöschl, G., Goodrich, D. C., Gupta, H. V., Sivapalan, M., Tachikawa, Y., Troch, P. A., and Weiler,
1274 M.: A synthesis framework for runoff prediction in ungauged basins, in: Runoff Prediction in Ungauged Basins,
1275 Cambridge University Press, 11–28, https://doi.org/10.1017/CBO9781139235761.005, 2013.

1276 Ye, S., Yaeger, M., Coopersmith, E., Cheng, L., & Sivapalan, M. (2012). Exploring the physical controls of
1277 regional patterns of flow duration curves–Part 2: Role of seasonality, the regime curve, and associated process
1278 controls. Hydrology and Earth System Sciences, 16(11), 4447-4465.

1279 Yokoo, Y. and Sivapalan, M.: Towards reconstruction of the flow duration curve: Development of a conceptual
1280 framework with a physical basis, Hydrol. Earth Syst. Sci., 15, 2805–2819, https://doi.org/10.5194/hess-15-2805-
1281 2011, 2011.

1282